Submerged reef terraces in the Maldivian Archipelago (Indian Ocean)

Alessio Rovere[1,2,3], Pankaj Khanna[4], Carlo Nike Bianchi[5], André W. Droxler[4], Carla Morri[5], David F. Naar[6]

1 MARUM, University of Bremen, Bremen, Germany, arovere@marum.de

2 ZMT, Leibniz Center for Tropical Marine Research, Bremen, Germany

3 Lamont-Doherty Earth Observatory, Columbia University, Palisades, NY, USA

4 Department of Earth, Environmental and Planetary Sciences, Rice University, Houston, TX 77005, USA

5 DiSTAV (Department of Earth, Environment, and Life Sciences), University of Genoa, Genova, Italy

6 College of Marine Science, University of South Florida, St. Petersburg, FL, USA

Abstract

Sea-level changes have shaped the world's carbonate platform margins and continental shelves, leaving typical geomorphic imprints, such as drowned reef terraces. In this paper, we present the results of 112 scuba diving transects across seven different Maldivian atolls and one multibeam survey around Malé Island, the capital of Maldives. We report on the occurrence of drowned reef terraces down to 120 m depth. In total, we identified six levels of submerged terraces that we consider as indicative of periods of time with stable or slowly rising sea level that can be attributed either to deceleration of the last deglacial sea-level rise or to Late Quaternary sea-level highstands. We compare our dataset to the depth of reef terraces reported globally, and we discuss the reasons why common global submerged terrace levels are difficult to identify in the field record.

Keywords

Submerged reef terraces; Maldives; Multibeam bathymetry; Scuba diving

Introduction

Since the early work of Darwin (1842), coral reefs have captured the interest of ecologists and geologists, who attempted to explain their formation (Braithwaite et al., 1973), morphology (Stoddart, 1969a), the relationships between ecological and geomorphological features (Lasagna et al., 2010a), and the inheritance of landforms from past sea levels (Schlager, 2005; Montaggioni and Braithwaite, 2009). The Maldives represent the archetype of an atoll reef archipelago (Naseer and Hatcher, 2004) and, as such, are a good example of modern atoll morphology (Aubert and Droxler, 1992, 1996; Purdy and Bertram, 1993; Risk and Sluka, 2000; Belopolsky and Droxler, 2004; Morri et al., 2015).

Recent geomorphological studies on the Maldivian reefs aimed to constrain their Holocene/uppermost Pleistocene inherited features (Gischler et al., 2008; Klostermann et al., 2104), the role of environmental factors (such as wave energy or coral growth) in shaping island morphology (Kench et al., 2006, 2009), the development of sub-aerial karst morphologies during intervals of low sea level (Colantoni et al., 2003), and the effects of human impacts on coral reef geomorphology (Brown and Dunne, 1988).

Similar to other continental shelves, both in tropical (Blanchon and Jones, 1995; Blanchon, 2011) and non-tropical areas (Rovere et al., 2011; Zecchin et al., 2015), earlier studies reported that the Maldives are characterized by submerged terraces from few meters below present sea level to 130 m depth (Bianchi et al., 1997; Anderson, 1998; Colantoni et al., 2003; Fürstenau et al., 2009; Rufin-Soler et al., 2013). Blanchon and Jones (1995), among others, attributed the formation of submerged reef terraces to periods of stable or slowly rising sea level, built by the interplay between coral reef growth and marine erosion near sea level. More recent studies also highlighted that reef terraces could also form contextually to rapid sea-level rise events by reef back-stepping (Schlager, 2005; Khanna et al., 2017).

In this study, we present the results of 112 scuba diving transects, at 7 different Maldivian atolls. We integrate our scuba surveys with the results of a high-resolution multibeam survey acquired around Malé Island upper slope, part of the southeastern rim of North Malé Atoll. We identify six levels of submerged reef terraces, from ~25 to ~106 m below present sea level, that are widespread in the Maldivian Archipelago. We discuss the possible mechanisms and timing of their formation, and we analyze them in the broader context of reef terraces reported globally.

Materials and Methods

Geological and Ecological Setting

The Maldivian Archipelago consists of a double chain of 22 atolls stretching over more than 800 km from 7°04' N to 0°48' S and centered around 73° E in the Indian Ocean (Fig. 1a). The Maldivian atolls represent the top of one of the largest modern carbonate platforms and constitute the central and largest part of the Chagos-Laccadives ridge (Risk and Sluka, 2000). As the Maldives platform has been far from any terrigenous influence for its 50 Ma-long history, this 2-3 km-thick edifice is composed entirely of carbonate sediments. These modern atolls are part of the latest phase in the evolution of this platform, which initially established itself on top of an early Eocene subsiding volcanic plateau (Aubert and Droxler, 1992, 1996; Purdy and Bertram, 1993; Belopolsky and Droxler, 2004).

Three distinct intervals have been identified in the Cenozoic stratigraphic evolution of the Maldivian carbonate system, corresponding to the Palaeogene (Eocene to late Oligocene), the Neogene (early Miocene to early Pliocene), and the late Pliocene-Pleistocene (Aubert and Droxler, 1996). Eustatic sea-level changes in the last 3 Ma triggered increased karstification of the reef framework, which is speculated to form the morphology inherited by the modern reefs (Purdy and Bertram, 1993; Colantoni et al., 2003; Gischler et al., 2014). The Holocene history of Maldivian (among other Indo-Pacific) coral reef systems has been summarized by Montaggioni (2005), mostly based on Woodroffe (1992, and references therein). The degree of modern reef development appears to be linked to coral community structure. Communities consisting principally of branching and domal corals underwent substantial accretion and produced well-developed reefs, whereas assemblages comprising of foliaceous and encrusting corals produced only incipient reefs (Bianchi et al., 2017). The highest accretion rates (up to 20 $mm \cdot a^{-1}$) were measured for tabular and aroborescent acroporids (Perry and Morgan, 2017b).

At the Last Glacial Maximum (LGM), from 23 to about 19 ka BP, reefs only developed along what were to become the fore slopes of present reefs, forming accumulations a few meters thick at vertical rates of up to 1 mm·a^{-1} (Kleypas, 1997; Montaggioni, 2005). The rapid postglacial rise in sea level, from about 19 to 6.5 ka BP, was accompanied by the settlement of three successive reef generations, within the periods 17.5-14.7, 13.8-11.5 and 10 ka BP to the present. From the LGM to the early Holocene, coral settlement has probably declined (Montaggioni, 2005).

In the Maldives, Holocene reef growth started as early as 8.5 ka BP (Gischler et al., 2008). Marginal reefs, dominated by robust branching corals and coralline algae, accreted in the 'keep-up' mode at rates of 15 m·ka^{-1}. Rate of sea-level rise slowed significantly from 7-6 ka BP and subsequently gradually rose at rates of 1 m·ka^{-1}. Lagoon reefs, characterized by domal corals and detrital facies, accreted in the 'catch-up' mode at rates of 0.25 to 1 m·ka^{-1} (Gischler et al., 2008). Recent estimates on living reefs indicate that the bioconstructional potential of oceanic reefs is higher than that of lagoon reefs; however, both were able to exhibit superstratal bioconstruction in undisturbed conditions (Bianchi et al., 2017). The overall Holocene reef thickness is generally less than 20 m (Kench et al., 2009; Morri et al., 2015). Submarine cementation in Holocene reefs is rather weak, presumably as a consequence of high accretion rates, i.e., short time available for consolidation (Gischler et al., 2008). Present-day living reefs exhibit similar features (Lasagna et al., 2010a; Morri et al., 2010). While information on bioerosion rates in Maldivian coral reefs is not available, recent field work showed abundant clionaid sponges on dead massive corals (Lasagna et al., 2008; Bianchi et al., 2017). This suggests that bioerosion rates might be particularly high.

Some studies on the topography of Maldivian reefs are available in the literature. The shallow (<130 m depth) submarine geomorphology of Ari atoll was investigated using multibeam sonar (Fürstenau et al., 2009), with the result of detailing the knowledge of submerged reef terraces that were previously recognized solely on the basis of single beam (Anderson, 1998) or scuba diving (Morri et al., 1995; Bianchi et al., 1997) surveys in localized areas of the archipelago. In general, studies of the Maldives atoll upper slopes have recognized breaks in slope at recurrent depths in Ari (14 dive surveys, Morri et al., 1995, and 2 multibeam profiles, Fürstenau et al., 2009) and Felidhoo (13 scuba transects, Bianchi et al., 1997) atolls. An abrupt break in the reef slope at ~130 m below present sea level has been associated to the Last Glacial Maximum (LGM) sea-level position

(Anderson, 1998; Fürstenau et al., 2009).

The earliest studies of Maldivian reef ecology date back to the turn of the 20th century (Gardiner, 1901-1905; Agassiz, 1903), but thorough field investigations on coral communities started with the Xarifa expedition in the late 1950s (Wallace and Zahir, 2007). References for the ecology of Maldivian coral reefs are provided by Andréfouët (2012) and by Morri et al. (2015). Research on coral zonation highlighted the dominance of tabular and branching acroporid corals, which are responsible for superstratal growth and rapid accretion, in shallow water (Davies et al., 1971; Scheer, 1972, 1974; Risk et al., 1994; Lasagna et al., 2010b); below 20 m the only significant bioconstruction was due to the azooxanthellate tree coral *Tubastraea micranthus* (Morri et al., 1995; Bianchi et al., 1997). Overall, bioconstructional capacity of Maldivian coral reefs has been shown to be high through a century of research. However, recent ecological crises resulting from major bleaching episodes, outbreaks of the corallivorous crown-of-thorn starfish *Acanthaster planci*, and other disturbances (Bianchi et al., 2006; Morri et al., 2010, 2015; Lasagna et al., 2014; Saponari et al., 2015; Pisapia et al., 2016) reduced bioconstructional capacity (Bianchi et al., 2017) and drew attention to the risk of platform drowning (Ciarapica and Passeri, 1993). The 2016 bleaching event severely impacted the coral communities of the Maldives (Perry and Morgan, 2017a), leading to a collapse in reef accretion potential and carbonate budgets (Perry and Morgan, 2017b).

Scuba Diving Transects

In this study, we focus on the reef slopes of seven Maldivian atolls (Fig. 1a): Ari, Felidhoo, North Malé, South Malé, Rashdoo, Suvadiva, and Thoddhoo. Across their margins, we surveyed a total of 112 scuba diving transects (see Supplementary Data for the location and data collected for each scuba survey). Depth measurements were corrected for tidal variability according to local tidal predictions by the Hydrographic Office (Malé Island) and referred to chart datum. In the central atolls, tidal range is generally between 0.3 to 0.7 m (Fürstenau et al., 2009). The transects were surveyed over a temporal interval between 1997 and 2013. Due to the long time span encompassed by our dataset, it is possible that the terrace morphologies were subject to minor inter-annual variations caused by debris flows and sedimentation.

During the scuba surveys, we started each transect from the deepest reachable part of the reef and took notes along a path perpendicular to the shoreline until the shallower part of the reef. In general, the transects ended on either the reef flat (Fig. 2), at 2-3 m depth, or on the upper terrace on the reef front (Fig. 2). Coordinates of each dive site were obtained before the dive with a Garmin handheld GPS or extracted from nautical charts. We estimate that the horizontal accuracy of the positioning is in the range of few tens of meters. Before each dive, the type of reef (inner, that is in the lagoon, or outer, that is facing the ocean, Fig. 3b) was annotated, and during each dive we surveyed the prominent topographic and geomorphic features along the transect (Bianchi et al., 2004; Rovere et al., 2011).

In particular, we measured the depth of the modern reef flat or upper terrace (Fig. 2), the depth of submerged reef terraces (both on the inner and outer reefs, Fig. 2), and the depth of the base of coral rubble deposits (Fig. 2), which accumulate with a slope angle of 25-35°. Distances were measured with a 200 m-long graduated tape or with personal dive sonar (PDS, i.e., a device that allows one to measure distances underwater based on the round-trip time for an acoustic pulse to reflect off an object), and depths were measured with a diving computer (depth accuracy between 0.4 to 3 m, Rovere et al., 2010; Azzopardi and Sayer, 2012) or with PDS. Slope and directions were measured using a handheld clinometer (~5° accuracy) and a diving compass (~5° accuracy).

We estimated, through repeated measurements of the same points during scuba surveys, that the depths we measured carry a vertical uncertainty less than ±1 m. In order to calculate the modal depth of terraces in the Maldivian Archipelago, we describe each data point (e.g., terrace depth) collected during scuba surveys as Gaussian with $1\sigma=1$ m, in order to account for measurement errors. Then, we sum all the individual Gaussians to create a composite probability density function graph (the result is shown in Fig. 6b). Peaks in the composite probability density function are interpreted as modal depths where terraces are most likely to be found.

Multibeam Bathymetry

A high-resolution 300 kHz multibeam bathymetry and backscatter dataset was acquired in summer 2008 using a Kongsberg EM 3000 system integrated with an Applanix

Pos/MV navigation and motion system (Wright et al., 2002; Wolfson et al., 2007; Mallinson et al., 2014). The merged system provides 127 1.5°× 1.5° overlapping beams at a pulse width of 0.15 ms within a 130 degree swath. The differential GPS position accuracy of the bathymetry was ~1.0 m with a depth resolution of ~1 cm and depth accuracy of 5-10 cm. The bathymetric data were processed using the software CARIS HIPS. An underwater pressure sensor was deployed in the southwestern portion of Malé Island harbor and used to correct for sea-level variations due to tide and wind during the multibeam survey (Wolfson et al., 2007). An approximation of the MLLW (Mean Lower Low Water) sea level chart datum was established by using the lowest sea level recorded over the 8-day period (Wolfson et al., 2007). The survey surrounded Malé Island (Fig. 1c) including the southeastern corner of the North Malé Atoll (Fig. 1b).

The multibeam survey covers minimum water depths of about 1 m and reaches water depths beyond the slope break, often coinciding with a prominent break in slope at ~120 m on the southern margin. The southern margin quickly reached depths of ~150 m, at which the 300 kHz multibeam system was unable to receive return acoustic signals due to the attenuation caused by the warm saline waters of the area. This attenuation is evident in the data gaps that appear in water depths greater than ~130 m in the detailed multibeam bathymetry (Fig. 5c,d). Similarly, attenuation data gaps were observed in the warm saline waters around American Samoa with the same multibeam system (Wright et al., 2002). The multibeam survey reaches down to 50-60 m water depth on the northern, western, and eastern margins (Fig. 5a,b for details). These margins represent the inner lagoon of North Malé Atoll. In addition, the survey extends about 1 km west and 600 m north of Malé Island and covers the channels separating Malé from Funadhoo and Hulhule Islands (see Fig. 5a for details). To identify geomorphic features from this dataset, slope gradient maps were overlapped with bathymetric maps and the edges of reef terraces were traced as vectors in ArcGIS.

A series of twelve multibeam transects on the southern margin were selected at different depths to identify terraces from the shallowest parts of the area down to ~120 m depth. Hypsometric curves were plotted to identify the terraces at different depths. Minimum-maximum depth values for each terrace were identified from the examination of all twelve transects. To define the depth of a terrace and its associated uncertainty, we chose the median value and calculated the difference between the median value and the maximum or minimum depths.

Calculation of Paleo Relative Sea Level

To calculate the position of paleo relative sea level (RSL) from the depth of one terrace, it is necessary to estimate the position of sea level at the time when the terrace was forming. To do this, we use the concept of 'modern analog', which is often used in paleo sea-level reconstructions both at Holocene and older timescales (Van de Plassche, 2013; Shennan, 2015; Rovere et al., 2016). This concept is rooted in the principle of uniformitarianism, which applied to sea-level science would suggest that the environment of formation of a given landform is the same today as in the past.

In this study, we consider the reef flat or the upper terrace (Fig. 2) of modern reefs as the modern analog for the reef terraces that we observe at higher depths across the Maldivian Archipelago. Therefore, knowing the depth of a submerged terrace and the depth of the modern reef flat or upper terrace, we can reconstruct the paleo relative sea level (RSL) using this simple formula:

$$RSL = RTd - MAd \qquad \textbf{Eq.1}$$

where *RTd* is the measured depth of reef terrace and *MAd* is the water depth at which the modern analog is found today. The scuba data suggest that in the Maldives *MAd* is 6.1±2.6 m (see results).

The total uncertainty (σRSL) associated with the paleo RSL is obtained by adding individual errors in quadratic:

$$\sigma RSL = \sqrt{\sigma RTd^2 + \sigma MAd^2} \qquad \textbf{Eq.2}$$

Global Database of Coral Reef Terraces

The database presented in Fig. 9 and annexed as online Supplementary data has been assembled from studies reporting depths of reef terraces. The data were extracted from literature following this simple approach: 1) if the study reported depths as ranges we averaged the depth ranges and calculated their standard deviation (e.g., statements such as '*a terrace is found between 20 and 25 m*' were inserted in the database as one terrace at 22.5±2.5 m); 2) uncertainties from literature were kept as reported; 3) if no uncertainties were reported, no uncertainty value was inserted in the included database (this represents the majority of the cases).

Results

Scuba Diving Transects

In the seven atolls investigated (Fig. 1a), the results obtained from the scuba diving transects show that the morphology of Maldivian reefs is characterized by sets of reef terraces at recurrent depths (Fig. 3a). The same morphology can be found either on the outer reefs, facing the open ocean, or in inner reefs, facing the inner atoll (1 and 3, respectively, in Fig. 3b). In the next paragraphs, we describe the different morphological elements that have relevance in terms of paleo RSL.

The reef flat/upper terrace. In the Maldives, the shallow-water portion of the reef developing from the reef crest towards the inner lagoon and the outer ocean has the morphology of a flat, shallow-water terrace (Fig. 3a,c), which ends in a sub-vertical mid-shelf slope (Fig. 3d). This part of the reef is the most affected by modern constructional and erosional processes. The scuba diving datasets indicate that the average depth of the modern reef flat (inner reefs, Fig. 2) is 5.2±2.1 m. The average depth of the upper terrace (outer reefs, Fig. 2) is instead 6.5±2.7 m. Overall, the average depth of the modern edges of reef flats and upper terraces (*MAd*, see methods) is 6.1±2.6 m.

Terrace T1. The mid-shelf slope is interrupted by a first terraced surface (T1, Fig 3a, Fig. 4c,d,e,g) at a depth of 33 m. This terrace is characterized by a large depth span across the Maldivian Archipelago (±8 m). Often, the inner margin of this terrace is covered by accumulations of coral rubble deposits (Fig. 3a,d), only partially cemented by coralline algae. The rockfall deposits create a slope of ~25-30°, and their toe is located at ~25 m depth on average (dashed line in Fig. 6b). The outer edge of T1 is often sharp and ends in another abrupt break in slope (Fig. 3e).

Terraces T2 and T3. While terrace T1 extends in general for 10-20 m and represents an interruption of the mid-shelf slope, two other levels of terraces characterize the investigated coral reefs between 50 and 60 m depth. The shallowest level is represented by T2, at 50±2.5 m (Fig. 4b,d), followed by T3 at 58.8±3.8 m (Fig. 4c). These terraces are separated by relatively short but almost vertical cliffs and are often 40-60 m wide. The break in slope characterizing these deeper terraces is, therefore, better marked than that of T1 and is less masked by debris at the toe of the slope; however, these terraces are usually covered by a thin veneer of coralline sands.

Terrace T4. The deepest terrace found in a consistent number of scuba transects is T4, at 71.5±6 m (Fig. 4a,e,f,g). This terrace is usually up to 30-50 m wide (Fig. 4f).

Multibeam Bathymetry

The 2008 multibeam data sets (Fig. 5) show that the southern margin of Malé Island (extending to the southeastern corner of Malé Atoll) is characterized by several morphologically distinct sets of terraces, all shallower than 120 m. A total of nine terraces, named M1-M9, have been identified.

Terraces M1 – M4. The shallower reef terraces are located at 25±2 m (M1), 29.5±1.5 m (M2), 34.5±1.5 m (M3), and 38±2 m (M4). These were observed on the southern margin of Malé Island (Fig. 5c,e). These terraces are closely spaced along most of the southern margin. They can be clearly identified in the multibeam bathymetric dataset on the southwestern and southeastern corner of Malé Island (Fig. 5c,e).

Terrace M5 and M6. These two terraces are found at 46±4 m (M5) and 56±4 m (M6) (Fig. 5c,d,f). These terraces are wider than M1-M4, and they find a counterpart in T2 and T3 identified by scuba diving transects (Fig. 6b).

Terrace M7 and M8. The depths of these terrace levels are 70.5±5.5 m (M7) and 88.5±3.5 m (M8) (Fig. 5d,f,g). M7 correlates well to the terrace T4 identified by scuba diving transects, while M8 occurs at a depth where scuba diving was not attempted (Fig. 6b); however, measurements taken with PDS by divers at shallower depths provided quite consistent results (Fig. 4f,g).

Terrace M9. This is the deepest terrace identified by multibeam bathymetry, lying at a depth of 106.5±3.5 m (Fig. 5d,g). It is narrow and bounded by two steep cliffs, clearly visible in the bathymetry data.

The multibeam bathymetry also shows a distinct break in slope at ~120 m depth (Fig. 5c,d,g,). Moreover, the channel sea floor, separating Malé Island from Hulhule International Airport Island and Funadhoo Island (Fuel Depot Island), ranging in water depths from 40 to 60 m, displays a series of enclosed and unfilled round to oval depressions, typical of karst dissolution morphologies (sinkholes) (Fig. 5a,b). This typical karst morphology clearly illustrates that the North Malé Atoll lagoon floor was exposed when sea level was below 40-60 m as recently as during Marine Isotope Stages 3 and 2.

Paleo Relative Sea Level

In the scuba diving and multibeam surveys, we identified six general levels of submerged terraces in the Maldivian Archipelago (Fig.6 a-c). Starting from these average terrace depths (Fig. 6b), we used Eq.1 and Eq.2 to calculate paleo RSL at the time of terrace formation. In Table 1, we report the calculation of the paleo RSL depth and associated uncertainty from Eq.1 and Eq.2 for the terraces T1-T4 and M1-M9 (also represented in Fig. 6c).

Discussion

Depth of Maldivian Reef Terraces

The scuba diving and multibeam surveys confirmed earlier reports that several levels of drowned reef terraces are imprinted in the insular shelves of the Maldives (Morri et al., 1995; Bianchi et al., 1997; Anderson, 1998; Fürstenau et al., 2009; Rufin-Soler et al., 2013). While former studies were limited to few specific atolls, our data span most of the archipelago. In first instance, it is worth noting that the depths of the terraces identified through scuba diving transects (Fig. 6a,b) show a good match with those identified in the multibeam bathymetry of the southeastern corner of Malé Atoll (Fig. 6c). In general, the terraces M1 to M4 identified in the shallower areas provide further details on the terrace T1 identified in the scuba transects. M5, M6, and M7 show a good fit with T2, T3, and T4, respectively.

For the shallowest areas, T1 (M1-M4) is found across a large depth range throughout the archipelago. This terrace, which in most transects has a limited width, serves as base for coral rubble deposits, eroded and transported from the upper part of the reef front towards deeper parts of the reef (dashed line in Fig. 6b). Given its limited depth, it is possible that the large depth span of T1 (M1-M4) can be explained by differential reef growth or erosion at the wave base, which differs from site to site along the archipelago. The multibeam bathymetry data support this hypothesis, as they show that this feature is substantially more morphologically complex than the other terraces identified in this study (Fig. 5c). In further support of the dynamic character of the shallower terrace level, we highlight that, three years after the mass coral mortality of 1998, the large amount of newly generated coral rubble had obliterated many morphologies previously visible on the reef slope of the Maldives (Morri et al., 2015). Previous studies pointed out to the presence, at the same depth of T1, of several notches and caves (Bianchi et al., 1997; Rufin-Soler et al., 2013), which were tentatively correlated to periods of brief Holocene sea-level standstills.

T1 is probably still affected by modern geomorphic and ecological processes, and most likely underwent morphological changes in the last part of the Holocene (i.e., since 5-6 ka) when the pace of global Holocene sea-level rise slowed down and settled around its modern value (e.g., curve in Fig.7b, Lambeck et al., 2014). Despite this caveat, we retain T1 among the sea-level indicators due to its prominence and its widespread character. Further work, including age constraints, would be needed to understand the mechanisms of formation and morphological evolution of this terrace, as well as its relation to former sea levels.

The depths of terraces T2 (M5), T3 (M6) and T4 (M7) are recurrent in the seven atolls investigated (Fig. 6a,b) and correspond well with those identified in the Maldives by previous studies (Morri et al., 1995; Bianchi et al., 1997; Rufin-Soler et al., 2013) (Fig. 6d). The only difference we highlight with respect to the data of Bianchi et al. (1997) is that we attribute the large modal value that they identify at 20/25 m to accumulation of coral rubble at the toe of T1 (M1-M4) rather than to a terrace level.

Two other terraces (M8 and M9) are found at 88 and 106 m, respectively. These two terraces were identified by this study only in Malé, but their depth is consistent with earlier reports that at least three terraces characterize the deeper Maldivian slopes (below 80 m depth). In fact, Colantoni et al. (2003) suggested that the Maldivian atolls are characterized by a terrace at about 85 m, which also coincides with the bottom of the Blue Hole in Ari Atoll. This depth is consistent with our M8 terrace. Offshore Ari, two terraces were identified by multibeam surveys at 94 and 97 m (Fürstenau et al., 2009). These depths, despite being slightly shallower than M9, might be correlated to this terrace. Due to limitations in scuba diving, depths greater than 70-75 m were reached only in few dives. In South Malé atoll (Fig. 1b), one dive identified a terraced surface at 82 m, which, although slightly out of the depth range of T4 (M7), could be related to it. A deeper terrace, at 87 m (Fig. 4g) was instead identified in Suvadiva atoll (Fig. 1a), and correlates well with terrace M8. The deepest scuba observation was made in Rasdhoo Atoll (Figs. 1a, 3f). Here it was possible to identify a break in slope at 95 m. Due to the considerable depth, it was impossible to verify the lateral continuity of this terrace, therefore this point has not been considered in the terrace analysis shown in Fig. 6b. Nevertheless, we note that the depth of this terrace is just slightly deeper than M9.

Deeper terraces had been identified in the Maldives by multibeam surveys at 125±3 m (Fürstenau et al., 2009) and by single beam sonar at 130±10 m (Anderson, 1998). These correspond to a wide planar surface we identified in the multibeam surveys at a depth of ~120 m (Fig. 5c,d,e). This surface was interpreted by previous authors as being created during the Last Glacial Maximum (~21 ka).

Other prominent features that characterize the sea bottom of the Malé islands are related to karst morphologies that have been drowned by sea level during the last deglaciation. Such karst morphologies are mostly observed in the channel between Malé and Hulhule Islands (Fig. 5b) where Holocene sediments cannot accumulate due to strong tidal currents in this narrow channel. The depth of these irregular depressions is 50-60 m, and is similar to other water-filled karst features, such as the Blue Hole (Colantoni et al., 2003), observed in the Maldivian Archipelago (Fig. 5b). According to global eustatic sea-level curves (Grant et al., 2014), the channel between Malé and Hulhule Islands might have been exposed to subaerial agents several times at least during the last 150 ka. Therefore, it is likely that the karst morphology observed today has developed during this time frame.

Uncertainties in Paleo Relative Sea-Level Determinations

In Table 1, we present the results of the application of modern analog values (i.e., the depth of the modern reef flat or upper terrace) to the recorded depth of reef terraces in the Maldives to calculate the paleo RSL and associated uncertainties correlated with each terrace. We remark that the modern reef flat value of 6.1±2.6 m (*MAd* in Eq.1 and 2) can be considered as reliable only for the terraces presented in this study, and it is consistent with previous data for Maldivian inner and outer reefs by Lasagna et al. (2010a). It would not be wise to apply this value to the study of reef terraces at other sites. Rather, we highlight that the study of paleo reef terraces should always be coupled with an investigation of modern reef morphologies. The *MAd* depends mostly on the balance between incoming wave energy and reef growth rates near modern sea level, therefore significant intra-site differences need to be taken into account when using the modern analog concept. The small difference between the depth of the edge of the modern reef flat between inner reefs (5.2±2.1 m) and outer reefs (6.5±2.7 m) found in this study justifies the choice of one single value of *MAd* (6.1±2.6 m) in the calculations.

Another potential issue that might affect the paleo RSL calculation, as described by Eqs.1 and 2, is that the reef terrace depth (*RTd*) measured today might misrepresent the original terrace depth at the time of formation. It is indeed possible that the original terrace depth was either higher or lower than the one we measure today due to bioconstruction, deposition of coral rubble at the toe of the slope, or bio- and mechanical erosion (see Fig. 8). In this study, we adopt the scenario 1 illustrated in Fig. 8, i.e., we assume that the location where we measure the depth of the reef terrace today corresponds to the original surface where it was shaped by the paleo RSL. This is a simplistic approximation, also dictated by the fact that we have no constraints on the timing of the terraces.

To give an order of magnitude on how the cases 2 and 3 shown in Fig. 8 might affect paleo RSL calculations, Holocene reef accretion rates from more than 60 sites globally average at ~4-5 $m \cdot ka^{-1}$ (Hubbard and Dullo, 2016, their Table 6.1). In the Maldives, values ranging between less than 1 $m \cdot ka^{-1}$ (Gischler et al., 2008; Klostermann et al., 2014) and up to 15 $m \cdot ka^{-1}$ (Gischler et al., 2008, for periods of Holocene rapid sea-level rise) have been reported. Fewer data are available for the planation rates of marine terraces, but they can be up to several meters per ka.

The thickness of coral rubble or sediments deposited at the toe of the cliff should be also subtracted from the measured depth of a reef terrace. During the surveys, we always considered as the inner margin the innermost part of the terrace with a low inclination (10-15º), noting in the scuba transects whether coral rubble deposits were covering the inner margin (e.g., Fig. 3e). While it is still possible that the depth of the measured inner margin is covered by coralline sands and coral rubble, this should only be a thin veneer upon the terraced surface.

Timing of Formation: Deglacial *vs.* Past Interglacials

When were Maldivian reef terraces formed? In absence of dating constraints, it is only possible to make two alternative hypotheses on the age of the reef terraces identified in this study.

The first hypothesis is that the terraces were created by either reef catch-up during rapid sea-level rise events (Schlager, 2005; Khanna et al. 2017) or by marine planation during periods of deceleration/pauses of the postglacial sea-level rise (i.e., since 20 ka) followed by meltwater pulses (e.g. Green et al., 2014; Liu et al., 2015) that caused sudden increases in the rate of sea-level rise (Fig. 7a,b). This hypothesis is the one favored by previous studies in the Maldives, which attribute submerged reef terraces to postglacial and Holocene reef growth on the Pleistocene foundation (Bianchi et al., 1997; Fürstenau et al., 2009; Rufin-Soler et al., 2013). One argument that supports the hypothesis that the reef terraces observed in this study were created since the LGM (Fig. 7a,b) is the observation that the terraces have widths most often included between 10 and 60 m. At rates of marine planation of 40-70 $m \cdot ka^{-1}$ (Blanchon and Jones, 1995), reef terraces such as the ones presented in this study would form in ~0.15-1.2 ka. This matches roughly the duration of the periods of deceleration of Holocene sea level rise shown in Fig. 7a (~0.2-1 ka). Recent studies also showed that, during periods of rapid sea-level rise, up to six terraces within 2 ka can develop as a result of back-stepping (Khanna et al., 2017).

The notion that submerged reef terraces were formed during the last deglaciation has been also proposed by previous studies, either through correlation with dated features such as relic reef build-ups (Blanchon et al., 2002) or through chronostratigraphy and correlation with other sites (Green et al., 2014). On the Texas shelf, the hypothesis that sudden accelerations of Holocene sea level have shaped carbonate platforms has recently been substantiated by rigorous data and radiometric age constraints (Khanna et al., 2017).

The second age hypothesis is that some or all of the submerged reef terraces described in this study were instead shaped by past sea-level highstands peaking below modern sea level (Fig. 7c), and the reef growth since the Last Glacial Maximum represents only a thin veneer upon these older surfaces. Past highstands that might have formed the terraces might include substages of MIS 7, MIS 5 and MIS 3 (see Siddall et al., 2007 for a review of eustatic sea-level position in these periods). If all the terraces described in this study were formed during the Pleistocene, then the question remains whether each terrace should be attributed to a single highstand or if the terraces represent different sea-level events within a single highstand.

Without further chronological constraints it is not possible to discern between these two hypotheses. At the present state of the art, most of the radiocarbon age constraints for reef formations in the Maldives are younger than ~8 ka (Gischler et al., 2008; Kench et al., 2009) (blue dots in Fig. 7b). In some case, radiocarbon dates may be complicated by the recycling of more recent radiocarbon, produced withi the reef setting. However, too much organic carbon would likely preclude reef growth. Using a ramped pyrolysis radiocarbon dating technique (e.g., Rosenheim et al., 2013) could potentially address the recycling of carbon if sufficient organic carbon was deposited during the reef formation at that time. A future feasibility study of using this technique in this tropical setting would appear warranted. We therefore remark that recent improvements in the precision of U-series disequilibrium dating (U-Th dating) should prove a more useful dating technique because it avoids the issue of radiocarbon recycling and also offers a greater age resolution than the shorter radiocarbon half-life dating technique (see Dutton, 2015, and references therein for a more complete discussion). One fragment of *Acropora* sp., collected in a core at 15 m depth on Rashdoo Atoll, was dated with the U-series disequilibrium technique to the onset of MIS 5e (136.9±2 ka) (Gischler et al., 2008). North of Rashdoo, in Maalhosmadulu Atoll, Kench et al., 2009 used U-series to date the last interglacial reef (122±7 ka) at 14.2 meters below present sea level.

Departures from Eustasy

In conjunction with paleo RSL calculations and age determinations, it is necessary to consider whether the reef terraces presented here underwent significant vertical movements since they were formed. In first approximation, there are two main factors that need to be considered: tectonics (e.g., Sugihara et al., 2003) and glacio-hydro isostatic adjustment (GIA) (e.g., Milne and Mitrovica, 2008). As both processes are timedependent, the unresolved issue of timing of formation allows us only to explore the sensitivity to our dataset to different scenarios of tectonics or GIA.

Regarding the tectonic factor, the Maldives have undergone long-term subsidence. Published subsidence rates vary between 0.035 $m \cdot ka^{-1}$ to 0.15 $m \cdot ka^{-1}$ since the onset of the last interglacial (Gischler et al., 2008). With the caveat that assuming linearity from long-term tectonic histories can be misleading, we show how these tectonic rates would affect eustatic sea-level curves in Fig. 7b,c (see gray band in both panels versus the dashed line, representing global eustatic sea level). As an example, a reef formed at 6 ka BP in the Maldives would be displaced downwards by 0.2-0.9 m. Similarly, a 21 ka BP reef would be displaced dwnwards by 0.7 to 3.2 m. Under the same long-term tectonic rates, a MIS 5e (deposited 125 ka ago) reef in the Maldives would have been displaced downwards 4 to 18 m. Any long-term subsidence estimate should also account for earth dynamic topography, in particular at timescales of hundred thousands of years (Austermann et al., 2017). For the Maldives, dynamic topography models predict from ~3 m of uplift to ~13 m of subsidence, the latter again in broad agreement with both long-term subsidence rates and the depth of dated last interglacial reefs (Gischler et al., 2008; Kench et al., 2009).

The GIA-related departure from eustasy has a slight latitudinal dependence in the Maldivian Archipelago (Morri et al., 1995). According to published GIA models (Milne and Mitrovica, 2008), a shoreline deposited 6 ka in the Maldives should have been displaced by -1.5 m in Rashdoo (north) and by -2 m in Suvadiva (south). Shorelines deposited 21 ka ago should be instead found 5.7 and 3.2 m (in Rashdoo and Suvadiva, respectively) below the eustatic value (Milne and Mitrovica, 2008). Also a Last Interglacial shoreline would be displaced in the Maldives due to GIA. The few models currently available for this region (Austermann et al., 2017) predict that a shoreline deposited in Rashdoo atoll 125 ka ago would be today 1.5±0.3 m higher than the MIS 5e eustatic value. The data presented above show that GIA and tectonics contributed several meters to the vertical displacement of the reef terraces described in this study, regardless of their age.

A Global Sequence of Submerged Reef Terraces?

As reported in the discussion above, submerged reef terraces are common features on tropical and subtropical atolls, barrier reefs, and continental shelves. In total, we identified 52 areas (including the Maldives) where levels of submerged reef terraces have been reported in literature (Fig. 9a-e). When plotting the depths of these reef terraces (Fig. 9f), we show that there is very little agreement towards common global levels. The reasons for this mismatch are evident from the points raised in the discussion of the Maldivian terraces. In summary, global levels of submerged reef terraces do not emerge because of the following reasons:

1. Fig. 1f compares depths of terraces and not paleo RSL. This is due to the fact that most studies do not report enough data on modern analogs to allow the use of Eq.1 and Eq.2 to properly calculate RSL and its related uncertainties.
2. Even if it would be possible to calculate paleo RSL from the terraces at each site, most reef terraces plotted in Fig. 9a-e do not have radiometric age constraints. To be able to compare terrace levels at different sites, it would be necessary to establish the age of each terrace level and account for departures from eustasy caused by GIA and/or tectonics. An example of the magnitude of GIA-induced departures from eustasy for a shoreline deposited 6 ka is shown in Fig. 9a-e using the GIA model results of Milne and Mitrovica (2008).
3. It is necessary to disentangle timing and mechanisms of formation, in order to understand which terraces formed during rapid sea-level rise events, or during decelerating events, or on top of topographic features developed during previous interglacials. Besides U-series or radiocarbon dating of the different terrace levels, one solution to disentangle different timings of formation is represented by the application of stratigraphic forward models at different time scales and with different sea level scenarios (Warrlich et al., 2002; Koelling et al., 2009; Barret and Webster, 2012; Seard et al., 2013; Camoin and Webster, 2015).

It is worth noting that, overall, age constraints are available for only few sites among those reported in the database (see Supplementary Materials). Where available, radiometric ages of superficial sediments collected above the terraces indicate a post-LGM age, and attribute the formation of the terrace to short periods of deceleration or pause of the sea-level rise since 21 ka BP (e.g., Nair, 1974; Vora and Almeida, 1990; Wagle et al., 1994). In general, only few studies in our database (e.g. Stanley and Swift, 1968; Gvirtzman, 1994) assume that the reef terraces might have formed during previous interglacial periods.

Conclusions

The results of the combined scuba and multibeam surveys in the Maldives, together with the comparison with other studies worldwide, allow us to draw three main conclusions.

1. On atoll upper slopes of the Maldivian Archipelago, six levels of submerged reef terraces are conserved between ~25 and ~106 m depth. These reef terraces are ubiquitous in the archipelago. These submerged reef terraces are indicators of paleo relative sea-level (RSL) positions. Comparisons with modern Maldivian reef flats show that, to calculate paleo RSL from the modern depth of a reef terrace, one should add at least ~6 m to the measured depth. Uncertainties on this estimate might be substantial, up to a few meters.
2. Several studies suggest that reef terraces similar to those presented here could be related to pauses or decelerations of sea-level rise since the Last Glacial Maximum, although, at least in the Maldives, the absence of chronologic constraints leaves the question open whether the terraces are instead relicts from past interglacials. Improving chronological constraints on these terraces remains therefore a central goal for future studies, both in the Maldives and elsewhere. With a more solid chronology for the reef terrace levels presented in this study, departures from eustasy might be calculated more precisely. Published GIA models and tectonic subsidence rates show that these processes might affect paleo RSL estimates by several meters.
3. Understanding the timing of formation of reef terraces such as those shown in this study is also important to gauge the sensitivity of ice sheets to sudden collapses. In fact, if the terraces were formed during slowdowns of the Holocene sea-level rise, they would have to be drowned under sudden sea-level accelerations to guarantee their preservation. Holocene sea-level reconstructions show that such patterns of deceleration-acceleration are indeed possible. The period between 11.4 and 8.2 ka is generally characterized by high sea-level rise rates (Lambeck et al., 2014, Fig.7 a,b),

punctuated by sudden decelerations that might have contributed to the creation of the deeper terraces. It has been proposed that a meltwater pulse (MWP-1C) happened ~8 ka BP, causing drowning of reef terraces formed before this period (Blanchon, 2011). Around 12 ka the eustatic sea-level curve of Lambeck et al. (2014, Fig.7 a,b) shows a deceleration in the sea-level rise, followed by MWP-1B (Bard et al., 2010) (starting at ~11.3 ka BP). Before this, a period of falling sea level (Lambeck et al., 2014, Fig.7 a,b) at ca. 15 ka was followed by a period of rapid sea-level rise at the onset of the Bølling Allerød warm period, coinciding with the MWP-1A (Liu et al., 2015). However, a recent study along the South Texas Shelf highlighted that reef terraces could also form contextually to rapid sea-level rise events by reef back-stepping during the Bølling Allerød warm period related to decadal or century-long ice sheet collapses (Khanna et al., 2017). The existence of nine terrace levels in the Maldives would suggest that the Holocene sea-level rise was punctuated by even more events such as those described above.

Acknowledgments

AR's research is supported by the Institutional Strategy of the University of Bremen, funded by the German Excellence Initiative (ABPZuK-03/2014); by ZMT, the Leibniz Center for Tropical Marine Ecology, Bremen and by the Deutsche Forschungsgemeinschaft (DFG) as part of the Special Priority Program (SPP)-1889 "Regional Sea Level Change and Society" (SEASCHANGE - RO-5245/1-1). The multibeam data presented in this study were acquired by DFN and AD, with extensive field and data processing support from Brian Donahue. AD was originally funded for this Maldives research by a NSF grant, award Number 0729070. Additional survey assistance was provided by Randi Naar and personnel from the Environmental Research Center (currently the Environmental Protection Agency, EPA) of the Republic of Maldives. Special thanks go to Gordon Ewers and Aishath Farhath Ali for their logistic assistance and to Hussain Ibrahim for his assistance at sea with the Captain and Crew from the EPA. Multibeam funding was provided by the EPA and the University of South Florida. Albatros Top Boat (Verbania, Milan and Malé) organized CNB, CM and AR’s scientific cruises in the Maldives: we thank Donatella ‘Dodi’ Telli and Massimo Sandrini for their support. The block diagram in Fig. 3a is derived by an original field sketch by Valeriano Parravicini (EPHE-CRIOBE, France). We thank Glenn Milne for providing the datasets used in Fig. 1A,B of Milne and Mitrovica (2008), to build Fig. 9 of this study. This study was motivated by discussions at PALSEA, a PAGES/INQUA working group.

References

Abbey, E.A., Webster, J.M., Beaman, R.J., 2011. Geomorphology of submerged reefs on the shelf edge of the Great Barrier Reef: The influence of oscillating Pleistocene sea-levels. Mar. Geol. 288, 61–78.

Acker, K.L., 1987. The Carbonate-siliciclastic facies transition in the modern sediments off the northeast coast of Barbados, WI.

Agassiz, A., 1903. The coral reefs of the Maldives. Mem. Museum Comp. Zool. Harvard Coll. 29, 1–168.

Anderson, R.C., 1998. Submarine topography of Maldivian atolls suggests a sea level of 130 metres below present at the last glacial maximum. Coral Reefs 17, 339–341.

Andréfouët, S. (Ed.), 2012. Biodiversity, resources, and conservation of Baa Atoll (Republic of Maldives) a UNESCO Man and Biosphere Reserve, Atoll Research Bulletin 590, 1-235.

Aubert, O., Droxler, A.W., 1996. Seismic stratigraphy and depositional signatures of the Maldive carbonate system (Indian Ocean). Mar. Pet. Geol. 13, 503–536.

Aubert, O., Droxler, A.W., 1992. General Cenozoic evolution of the Maldives carbonate system (equatorial Indian Ocean). Bull. Centres Rech. Explor. Elf Aquitaine 16, 113–136.

Austermann, J., Mitrovica, J.X., Huybers, P., Rovere, A., 2017. Detection of a dynamic topography signal in last interglacial sea level records. Sci. Adv. 3, e1700457.

Azzopardi, E., Sayer, M., 2012. Estimation of depth and temperature in 47 models of diving decompression computer. Underw. Technol. Int. J. Soc. Underw. 31, 3–12.

Bard, E., Hamelin, B., Delanghe-Sabatier, D., 2010. Deglacial Meltwater Pulse 1B and Younger Dryas Sea Levels Revisited with Boreholes at Tahiti. Science (80-.). 327, 1235–1237.

Barrett, W., 1962. Emerged and submerged shorelines of the Dominican Republic. Rev. Geogr. 51–77.

Barrett, S.J., Webster, J.M., 2012. Holocene evolution of the Great Barrier Reef: Insights from 3D numerical modelling. Sedimentary Geology, 265, 56-71.

Belopolsky, A. V, Droxler, A.W., 2004. Seismic expressions of prograding carbonate bank margins: Middle Miocene, Maldives, Indian Ocean. AAPG Special Volumes.

Bianchi, C.N., Ardizzone, G.D., Belluscio, A., Colantoni, P., Diviacco, G., Morri, C., Tunesi, L., 2004. Benthic cartography. Biol. Mar. Mediterr. 11, 347–370.

Bianchi, C.N., Colantoni, P., Geister, J., Morri, C., 1997. Reef geomorphology, sediments and ecological zonation at Felidu Atoll, Maldive islands (Indian Ocean), in: Lessios, H.A. and MacIntyre, I.G. (Eds.), Proceedings of the 8th International Coral Reef Symposium. Smithsonian Tropical Research Institute, Panamá, 1, pp. 431–436.

Bianchi, C.N., Morri, C., Lasagna, R., Montefalcone, M., Gatti, G., Parravicini, V., Rovere, A., 2017. Resilience of the Marine Animal Forest: lessons from Maldivian coral reefs after the mass mortality of 1998, in: Rossi, S., Bramanti, L., Gori, A., Orejas, C. (Eds.), Marine Animal Forests. Springer International Publishing, Cham, Switzerland, pp. 1241–1269. doi:10.1007/978-3-319-17001-5_35-1

Bianchi, C.N., Morri, C., Pichon, M., Benzoni, F., Colantoni, P., Baldelli, G., Sandrini, M., 2006. Dynamics and pattern of coral recolonization following the 1998 bleaching event in the reefs of the Maldives, in: Suzuki, Y., Nakamori, T., Hidaka, M., Kayanne, H., Casareto, B.E., Nadaoka, K., Yamano, H., Tsuchiya, M. (Eds.), Proceedings of the 10th International Coral Reef Symposium. Japanese Coral Reef Society, Tokyo, Japan, pp. 30–37.

Blanchon, P., 2011. Geomorphic zonation. Encyclopedia of Modern coral reefs Structure, form, Processes. doi:10.1007/978-90-481-2639-2

Blanchon, P., Jones, B., 1995. Marine-planation terraces on the shelf around Grand Cayman: a result of stepped Holocene sea-level rise. J. Coast. Res. 1–33.

Blanchon, P., Jones, B., Ford, D.C., 2002. Discovery of a submerged relic reef and shoreline off Grand Cayman: Further support for an early Holocene jump in sea level. Sediment. Geol. 147, 253–270. doi:10.1016/S0037-0738(01)00143-9

Braithwaite, C.J.R., Taylor, J.D., Kennedy, W.J., 1973. The evolution of an atoll: the depositional and erosional history of Aldabra. Philos. Trans. R. Soc. Lond. B. Biol. Sci. 266, 307–340. doi:10.1098/rstb.1973.0051

Brown, B.E., Dunne, R.P., 1988. The environmental impact of coral mining on coral reefs in the Maldives. Environ. Conserv. 15, 159–165.

Cabioch, G., Montaggioni, L., Frank, N., SEAWAY, Sallé, E., Payri, C., Pelletier, B., Paterne, M., 2008. Successive reef depositional events along the Marquesas foreslopes (French Polynesia) since 26 ka. Mar. Geol. 254, 18–34.

Camoin, G.F., Webster, J.M., 2015. Coral reef response to Quaternary sea-level and environmental changes: State of the science. Sedimentology, 62(2), 401-428.

Carrigy, M.A, Fairbridge, R.W., 1954. Recent sedimentation, physiography and structure of the continental shelves of Western Australia. Journal of the Royal Society of Western Australia 38, 65–95.

Chevalier, J.P., Denizot, M., Mougin, J.-L., Plessis, Y., Salvat, B., 1968. Etude géomorphologique et bionomique de l'atoll de Mururoa (Tuamotu). Cah. Pacifique 1–144.

Ciarapica, G., Passeri, L., 1993. An overview of the Maldivian coral reefs in Felidu and North Malé Atoll (Indian Ocean): Platform drowning by ecological crises. Facies 28, 33–65.

Colantoni, P., Baldelli, G., Bianchi, C.N., Capaccioni, B., Morri, C., Sandrini, M., Tassi, F., 2003. A cave flooded by marine water with hydrogen sulphide highlights the recent evolution of the Maldives (Indian Ocean): preliminary notes. Le Grotte d'Italia 4, 29–37.

Collins, L.B., 1988. Sediments and history of the Rottnest Shelf, southwest Australia: a swell-dominated, non-tropical carbonate margin. Sediment. Geol. 60, 15–49. doi:10.1016/0037-0738(88)90109-1

Darwin, C. R., 1842. The structure and distribution of coral reefs. Being the first part of the geology of the voyage of the Beagle, under the command of Capt. Fitzroy, R.N. during the years 1832 to 1836. London: Smith Elder and Co.

Davies, P.S., Stoddart, D.R., Sigee, D.C., 1971. Reef forms of Addu Atoll, Maldives Islands. Symp Zool Soc L. 28, 217–259.

Digerfeldt, G., Hendry, M.D., 1987. An 8000 year Holocene sea-level record from Jamaica: implications for interpretation of Caribbean reef and coastal history. Coral Reefs 5, 165–169.

Dullo, W.C., Camoin, G.F., Blomeier, D., Colonna, M., Eisenhauer, A., Faure, G., Casanova, J., Thomassin, B.A., 1998. Morphology and sediments of the fore-slopes of Mayotte, Comoro Islands: Direct observations from a submersible. Reefs carbonate platforms Pacific Indian Ocean. 217–236.

Dutton, A., 2015. Chapter 26: Uranium-thorium dating. In Handbook of Sea-Level Research, First Edition, Edited by Ian Shennan, Antony J. Long, and Benjamin P. Horton. 386-40

Fairbridge, R.W., Stewart Harris B, J., 1960. Alexa Bank, a drowned atoll on the Melanesian Border Plateau. Deep Sea Res. 7, 100–116.

Fletcher, C.H., Sherman, C.E., 1995. Submerged shorelines on O'ahu, Hawai'i: Archive of episodic transgression during the deglaciation? J. Coast. Res. 141–152.

Focke, J.W., 1978. Holocene development of coral fringing reefs, leeward off Curacao and Bonaire (Netherlands Antilles). Mar. Geol. 28, M31–M41. doi:10.1016/0025-3227(78)90091-9

Fricke, H.W., Landmann, G., 1983. On the origin of Red-Sea submarine canyons - Observations by submersible. Naturwissenschaften 70, 195–197. doi:Doi 10.1007/Bf01047561

Fürstenau, J., Lindhorst, S., Betzler, C., Hübscher, C., 2009. Submerged reef terraces of the Maldives (Indian Ocean). Geo-Marine Lett. 30, 511–515.

Gardiner, J.S. (Ed.), 1901-1905. The fauna and geography of the Maldive and Laccadive archipelagoes: being the account of the work carried on and of the collections made by an expedition during the years 1899 and 1900. University Press, Cambridge, UK, 1 (1) 1901, 1–138; 1 (2) 1903, 1–134; 1 (3) 1902, 1–148; 1 (4) 1903, 1–172; 2 (1) 1903, 1–144; 2 (2) 1903, 1–160; 2 (3) 1904, 1–168; 2 (4) 1905, 1–174.. doi:10.5962/bhl.title.10215

Gischler, E., Hudson, J.H., Pisera, A., 2008. Late Quaternary reef growth and sea level in the Maldives (Indian Ocean). Mar. Geol. 250, 104–113.

Gischler, E., Storz, D., Schmitt, D., 2014. Sizes, shapes, and patterns of coral reefs in the Maldives, Indian Ocean: The influence of wind, storms, and precipitation on a major tropical carbonate platform. Carbonates and Evaporites 29, 73–87. doi:10.1007/s13146-013-0176-z

Glynn, P.W., Veron, J.E.N., Wellington, G.M., 1996. Clipperton Atoll (eastern Pacific): oceanography, geomorphology, reef-building coral ecology and biogeography. Coral Reefs 15, 71–99. doi:10.1007/s003380050029

Goreau, T.F., Land, L.S., 1974. Fore reef morphology and depositional processes North Jamaica. Soc. Econ. Paleontol. Mineral. 77–89.

Grant, K.M., Rohling, E.J., Ramsey, C.B., Cheng, H., Edwards, R.L., Florindo, F., Heslop, D., Marra, F., Roberts, A.P., Tamisiea, M.E., others, Williams, F., 2014. Sea-level variability over five glacial cycles. Nat. Commun. 5, 5076. doi:10.1038/ncomms6076

Green, A.N., Cooper, J.A.G., Salzmann, L., 2014. Geomorphic and stratigraphic signals of postglacial meltwater pulses on continental shelves. Geology 42, 151–154.

Gvirtzman, G., 1994. Fluctuations of sea level during the past 400 000 years: the record of Sinai, Egypt (northern Red Sea). Coral Reefs 13, 203–214. doi:10.1007/BF00303633

Hengesh, J.V, Whitney, B.B., Rovere, A., 2011. A tectonic influence on seafloor stability along Australia’s north west shelf, in: 21st International Offshore and Polar Engineering Conference. Maui, HI, pp. 1–9.

Hine, A.C., Neumann, A.C., 1977. Shallow carbonate-bank-margin growth and structure, Little

Bahama Bank, Bahamas. Am. Assoc. Pet. Geol. Bull. 61, 376–406.

Houbolt, J.J., 1957. Surface sediments of the Persian Gulf near the Qatar Peninsula, Proefschrift Univ. Utrecht. Mouton.

Hubbard, D.K., Dullo, W., 2016. Coral reefs at the crossroads 6. doi:10.1007/978-94-017-7567-0

James, N.P., Ginsburg, R.N., 1979. The geological setting of Belize reefs. Seaward Margin Belize Barrier Atoll Reefs Morphol. Sedimentol. Org. Distrib. Late Quat. Hist. 1–14.

Johnson, D.P., Searle, D.E., 1984. Post-glacial seismic stratigraphy, central Great Barrier Reef, Australia. Sedimentology 31, 335–352. doi:10.1111/j.1365-3091.1984.tb00863.x

Kaye, C.A., 1959a. Geology of Isla Mona and notes on the age of Mona Passage., U. S. Geological Survey Professional Paper 317-CSP - 141.

Kaye, C.A., 1959b. Coastal Geology of Puerto Rico. US Government Printing Office.

Keating, B., 1985. Submersible observations on the flanks of Johnston Island (Central Pacific Ocean), in: Proceedings of the Fifth International Coral Reef Symposium. pp. 413–418.

Kench, P.S., Brander, R.W., Parnell, K.E., McLean, R.F., 2006. Wave energy gradients across a Maldivian atoll: Implications for island geomorphology. Geomorphology 81, 1–17.

Kench, P.S., Smithers, S.G., McLean, R.F., Nichol, S.L., 2009. Holocene reef growth in the Maldives: evidence of a mid-Holocene sea-level highstand in the central Indian Ocean. Geology 37, 455–458. doi:10.1130/G25590A.1

Khanna, P., Droxler, A.W., Nittrouer, J.A., Tunnell Jr, J.W., Shirley, T.C., 2017. Coralgal reef morphology records punctuated sea-level rise during the last deglaciation. Nat. Commun. 8, 1046. doi:10.1038/s41467-017-00966-x

Kleypas, J.A., 1997. Modeled estimates of global reef habitat and carbonate production since the last glacial maximum. Paleoceanography 12, 533–545. https://doi.org/10.1029/97PA01134

Klostermann, L., Gischler, E., Storz, D., Hudson, J.H., 2014. Sedimentary record of late Holocene event beds in a mid-ocean atoll lagoon, Maldives, Indian Ocean: Potential for deposition by tsunamis. Mar. Geol. 348, 37–43.

Koelling, M., Webster, J.M., Camoin, G., Iryu, Y., Bard, E., Seard, C., 2009. SEALEX—Internal reef chronology and virtual drill logs from a spreadsheet-based reef growth model. Global and Planetary Change, 66(1-2), 149-159.

Kühlmann, D.H.H., 1970. Die Korallenriffe Kubas. I. Genese und Evolution. Int. Rev. der gesamten Hydrobiol. Hydrogr. 55, 729–756.

Lambeck, K., Rouby, H., Purcell, A., Sun, Y., Sambridge, M., 2014. Sea level and global ice volumes from the Last Glacial Maximum to the Holocene. PNAS 111, 15296–15303. doi:10.1073/pnas.1411762111

Lasagna, R., Albertelli, G., Colantoni, P., Morri, C., Bianchi, C.N., 2010a. Ecological stages of Maldivian reefs after the coral mass mortality of 1998. Facies 56, 1–11. doi:10.1007/s10347-009-0193-5

Lasagna, R., Albertelli, G., Giovannetti, E., Grondona, M., Milani, A., Morri, C., Bianchi, C.N., 2008. Status of Maldivian reefs eight years after the 1998 coral mass mortality. Chem. Ecol. 24, 67–72. doi:10.1080/02757540801966454

Lasagna, R., Albertelli, G., Morri, C., Bianchi, C.N., 2010b. *Acropora* abundance and size in the Maldives six years after the 1998 mass mortality: patterns across reef typologies and depths. J. Mar. Biol. Assoc. United Kingdom 90, 919–922. doi:10.1017/S0025315410000020

Lasagna, R., Gnone, G., Taruffi, M., Morri, C., Bianchi, C.N., Parravicini, V., Lavorano, S., 2014. A new synthetic index to evaluate reef coral condition. Ecol. Indic. 40, 1–9. doi:10.1016/j.ecolind.2013.12.020

Liddell, W.D., Ohlhorst, S.L., Boss, S.K., 1984. Community patterns on the Jamaican fore reef (15-56 m). Paleont Am. 54, 385.

Liu, J., Milne, G.A., Kopp, R.E., Clark, P.U., Shennan, I., 2015. Sea-level constraints on the amplitude and source distribution of Meltwater Pulse 1A. Nat. Geosci. 9, 6–12. doi:10.1038/ngeo2616

Logan, B., 1962. Submarine topography of the Yucatan Platform. New Orleans Geological

Society.

Macintyre, I.G., 1967. Submerged coral reefs, west coast of Barbados, West Indies. Can. J. Earth Sci. 4, 461–474.

Mallinson, D., Hine, A., Naar, D., Locker, S., Donahue, B., 2014. New perspectives on the geology and origin of the Florida Middle Ground carbonate banks, West Florida Shelf, USA. Mar. Geol. 355, 54–70.

Milne, G.A., Mitrovica, J.X., 2008. Searching for eustasy in deglacial sea-level histories. Quat. Sci. Rev. 27, 2292–2302.

Moawad, M.B., 2013. Detection of the submerged topography along the Egyptian Red Sea Coast using bathymetry and GIS-based analysis. Egypt. J. Remote Sens. Sp. Sci. 16, 35–52. doi:10.1016/j.ejrs.2012.12.001

Montaggioni, L.F., 2005. History of Indo-Pacific coral reef systems since the last glaciation: Development patterns and controlling factors. Earth Sci. Rev. 71, 1–75.

Montaggioni, L.F., Braithwaite, C.J.R., 2009. Quaternary coral reef systems: History, development processes and controlling factors. Elsevier Science.

Morelock, J., Grove, K., Hernandez, M.L., 1983. Oceanography and patterns of shelf sediments, Mayaguez, Puerto Rico. J. Sediment. Res. 53, 371–381. doi:10.1306/212F81D9-2B24-11D7-8648000102C1865D

Morri, C., Aliani, S., Bianchi, C.N., 2010. Reef status in the Rasfari region (North Malé Atoll, Maldives) five years before the mass mortality event of 1998. Estuar. Coast. Shelf Sci. 86, 258–264.

Morri, C., Bianchi, C.N., Aliani, S., 1995. Coral reefs at Gangehi (North Ari Atoll, Maldive Islands). Publ. du Serv. Géologique du Luxemb. 29, 3–12.

Morri, C., Montefalcone, M., Lasagna, R., Gatti, G., Rovere, A., Parravicini, V., Baldelli, G., Colantoni, P., Bianchi, C.N., 2015. Through bleaching and tsunami: Coral reef recovery in the Maldives. Mar. Pollut. Bull. 98, 188–200. doi:10.1016/j.marpolbul.2015.06.050

Nair, R.R., 1974. Holocene sea-levels on the western continental shelf of India. Proc. Indian Acad. Sci. B 79, 197–203.

Naseer, A., Hatcher, B.G., 2004. Inventory of the Maldives coral reefs using morphometrics generated from Landsat ETM+ imagery. Coral Reefs 23, 161–168.

Newell, N.D., 1956. Geological reconnaissance of Raroia (Kon Tiki) Atoll, Tuamotu Archipelago: A revision of Bulletin 31 and Bulletin 36 of the Atoll Research Bulletin, Pacific Science Board, Washington, DC, November 30, 1954. Am. Museum of Natural History.

Perry, C.T., Morgan, K.M., 2017a. Post-bleaching coral community change on southern Maldivian reefs: is there potential for rapid recovery? Coral Reefs 36, 1189-1194. DOI 10.1007/s00338-017-1610-9.

Perry, C.T., Morgan, K.M., 2017b. Bleaching drives collapse in reef carbonate budgets and reef growth potential on southern Maldives reefs. Scientific Reports 7, 40581. DOI: 10.1038/srep40581.

Pisapia, C., Burn, D., Yoosuf, R., Najeeb, A., Anderson, K.D., Pratchett, M.S., 2016. Coral recovery in the central Maldives Archipelago since the last major mass-bleaching, in 1998. Scientific Reports 6, 34720. DOI: 10.1038/srep34720.

Poag, C.W., 1973. Late Quaternary sea levels in the Gulf of Mexico 394–400.

Purdy, E.G., Bertram, G.T., 1993. Carbonate concepts from the Maldives, Indian Ocean. AAPG Special Volumes.

Reches, Z., Erez, J., Garfunkel, Z., 1987. Sedimentary and tectonic features in the northwestern Gulf of Elat, Israel. Tectonophysics 141, 169–180.

Reiss, Z., Hottinger, L., 1984. The sea bottom—A mosaic of substrates. Gulf Aqaba 139–202.

Rigby, J.K., Roberts, H.H., 1976. Grand Cayman Island: geology, sediments and marine communities. Brigham Young University, Dept. of Geology.

Risk, M.J., Dunn, J.J., Allison, W.R., Horrill, C., 1994. Reef monitoring in Maldives and

Zanzibar: low-tech and high-tech science. Proc. Colloq. Glob. Asp. Coral Reefs, Miami, 1993 9, 66–72.

Risk, M.J., Sluka, R., 2000. The Maldives: A nation of atolls, in: Coral Reefs of the Indian Ocean: Their Ecology and Conservation. pp. 325–351.

Rosenheim, B.E., Santoro, J., Domack, E.W., 2013. Improving Antarctic sediment 14C dating using ramped pyrolysis: An example from the Hugo Island Trough. Radiocarbon. 55(1), 115-126.

Rovere, A., Parravicini, V., Vacchi, M., Montefalcone, M., Morri, C., Bianchi, C.N., Firpo, M., 2010. Geo-environmental cartography of the Marine Protected Area "Isola di Bergeggi" (Liguria, NW Mediterranean Sea). J. Maps 6, 505–519. doi:10.4113/jom.2010.1137

Rovere, A., Raymo, M.E., Vacchi, M., Lorscheid, T., Stocchi, P., Gómez-Pujol, L., Harris, D.L., Casella, E., O'Leary, M.J., Hearty, P.J., 2016. The analysis of Last Interglacial (MIS 5e) relative sea-level indicators: Reconstructing sea-level in a warmer world. Earth-Science Rev. 159, 404–427. doi:10.1016/j.earscirev.2016.06.006

Rovere, A., Vacchi, M., Firpo, M., Carobene, L., 2011. Underwater geomorphology of the rocky coastal tracts between Finale Ligure and Vado Ligure (western Liguria, NW Mediterranean Sea). Quat. Int. 232, 187–200. doi:10.1016/j.quaint.2010.05.016

Rufin-Soler, C., Mörner, N.-A., Laborel, J., Collina-Girard, J., 2013. Submarine morphology in the Maldives and Holocene sea-level rise. J. Coast. Res. 30, 30–40.

Saponari, L., Montano, S., Seveso, D., Galli, P., 2015. The occurrence of an *Acanthaster planci* outbreak in Ari Atoll, Maldives. Mar. Biodivers. 45, 599–600. doi:10.1007/s12526-014-0276-6

Sarano, F., Pichon, M., 1988. Morphology and ecology of the deep fore reef slope at Osprey Reef, (Coral Sea), in: Proceedings of the. 6th International Coral Reef Symposium, 2, pp. 607–611.

Scheer, G., 1974. Investigation of coral reefs at Rasdu Atoll in the Maldives with the quadrat method according to phytosociology, in: Proceedings of the 2nd International Coral Reef Symposium, Brisbane. pp. 655–670.

Scheer, G., 1972. Investigation of coral reefs in the Maldive Islands with notes on lagoon patch reefs and the method of coral sociology, in: Proceedings of the First International Coral Reef Symposium. pp. 87–120.

Schlager, W., 2005. Carbonate sedimentology and sequence stratigraphy. SEPM Soc for Sed Geology.

Seard, C., Borgomano, J., Granjeon, D. and Camoin, G., 2013. Impact of environmental parameters on coral reef development and drowning: Forward modelling of the last deglacial reefs from Tahiti (French Polynesia; IODP Expedition# 310). Sedimentology, 60(6), 1357-1388.

Shennan, I., 2015. Handbook of sea-level research. John Wiley & Sons Ltd, Chichester, UK, pp. 3–25. doi:10.1002/9781118452547.ch2

Siddall, M., Chappell, J., Potter, E.K., 2007. 7. Eustatic sea level during past interglacials. Dev. Quat. Sci. 7, 75–92.

Siddiquie, H.N., 1975. Submerged terraces in the Laccadive Islands, India. Mar. Geol. 18, 95–101. doi:10.1016/0025-3227(75)90045-6

Stanley, D.J., Swift, D.J.P., 1968. Bermuda's reef-front platform: bathymetry and significance. Mar. Geol. 6, 479–500.

Stoddart, D.R., 1969a. Ecology and morphology of recent coral reefs. Biol. Rev. 44, 433–498. doi:10.1111/j.1469-185X.1969.tb00609.x

Stoddart, D.R., 1969b. Geomorphology of the Marovo elevated barrier reef, New Georgia. Philos. Trans. R. Soc. Lond. B. Biol. Sci. 255, 383–402.

Sugihara, K., Nakamori, T., Iryu, Y., Sasaki, K., Blanchon, P., 2003. Holocene sea-level change and tectonic uplift deduced from raised reef terraces, Kikai-jima, Ryukyu Islands, Japan. Sediment. Geol. 159, 5–25. doi:10.1016/S0037-0738(03)00092-7

Tracey Jr, J.I., Ladd, H.S., Hoffmeister, J.E., 1948. Reefs of Bikini, Marshall Islands. Bull. Geol. Soc. Am. 59, 861–878. doi:10.1130/0016-7606(1948)59[861:ROBMI]2.0.CO;2

Tracey Jr, J.I., 1968. Reef features of the Caroline and Marshall Islands. Prof. Pap. US Geol. Surv. 600, 1–80.

Van de Plassche, O., 2013. Sea-level research: a manual for the collection and evaluation of data: A manual for the collection and evaluation of data. Springer. doi:10.1007/978-94-009-4215-8_15

Vora, K.H., Almeida, F., 1990. Submerged reef systems on the central western continental-shelf of India. Mar. Geol. 91, 255–262.

Wagle, B.G., Vora, K.H., Karisiddaiah, S.M., Veerayya, M., Almeida, F., 1994. Holocene submarine terraces on the western continental shelf of India: Implications for sea-level changes. Mar. Geol. 117, 207–225. doi:10.1016/0025-3227(94)90016-7

Wallace, C.C., Zahir, H., 2007. The “Xarifa” expedition and the atolls of the Maldives, 50 years on. Coral Reefs 26 (1), 3-5. doi:10.1007/s00338-006-0188-4

Warrlich, G.M.D., Waltham, D.A., Bosence, D.W.J., 2002. Quantifying the sequence stratigraphy and drowning mechanisms of atolls using a new 3D forward stratigraphic modelling program (CARBONATE 3D). Basin Research, 14(3), 379-400.

Wenke, F., Caiwang, B., Junren, C., Xitao, Z., 1982. Preliminary study on submarine relief of the northern South China Sea. Acta Oceanol. Sin. 4, 462–471.

Wilber, R.J., Milliman, J.D., Halley, R.B., 1990. Accumulation of bank-top sediment on the western slope of Great Bahama Bank: rapid progradation of a carbonate megabank. Geology 18, 970–974.

Williams, D.G., 1994. Marine habitats of the Cocos (Keeling) Islands. Atoll Res. Bull. 406, 1–11. doi:10.5479/si.00775630.406.1

Wolfson, M.L., Naar, D.F., Howd, P.A., Locker, S.D., Donahue, B.T., Friedrichs, C.T., Trembanis, A.C., Richardson, M.D., Wever, T.F., 2007. Multibeam observations of mine burial near Clearwater, FL, including comparisons to predictions of wave-induced burial. Ocean. Eng. IEEE J. 32, 103–118.

Woodroffe, C.D., 1992. Morphology and evolution of reef islands in the Maldives, in: Proceedings of the 7th International Coral Reef Symposium. pp. 1217–1226.

Wright, D.J., Donahue, B.T., Naar, D.F., 2002. Seafloor mapping and GIS coordination at America's remotest national marine sanctuary (American Samoa). Undersea with GIS 33–63.

Zecchin, M., Ceramicola, S., Lodolo, E., Casalbore, D., Chiocci, F.L., 2015. Episodic, rapid sea-level rises on the central Mediterranean shelves after the Last Glacial Maximum: A review. Mar. Geol. 369, 212–223.

Table 1. Depth of terraces in the Maldivian archipelago, calculation of paleo relative sea level and values used to estimate sediment cover and paleo water depth. See supplementary data, Eqs.1,2 and Fig. 1a for the calculations used to obtain the paleo relative sea level (RSL) estimates.

Name (SCUBA)	**Measured depth (RTd) ±σRTd (m)**	**RSL ±σRSL (m)**	**Name (Multibeam)**	**Measured depth (RTd) ±σRTd (m)**	**RSL ±σRSL (m)**
T1	33±8	26.9±8.4	M1	25±2	18.9±3.3
			M2	29.5±1.5	23.4±3
			M3	34.5±1.5	28.4±3
			M4	38±2	31.9±3.3
T2	50±2.5	43.9±3.6	M5	46±4	39.9±4.8
T3	58.8±3.8	52.7±4.6	M6	56±4	49.9±4.8
T4	71.5±6	65.4±6.5	M7	70.5±5.5	64.4±6.1
			M8	88.5±3.5	82.4±4.4
			M9	106.5±3.5	100.4±4.4

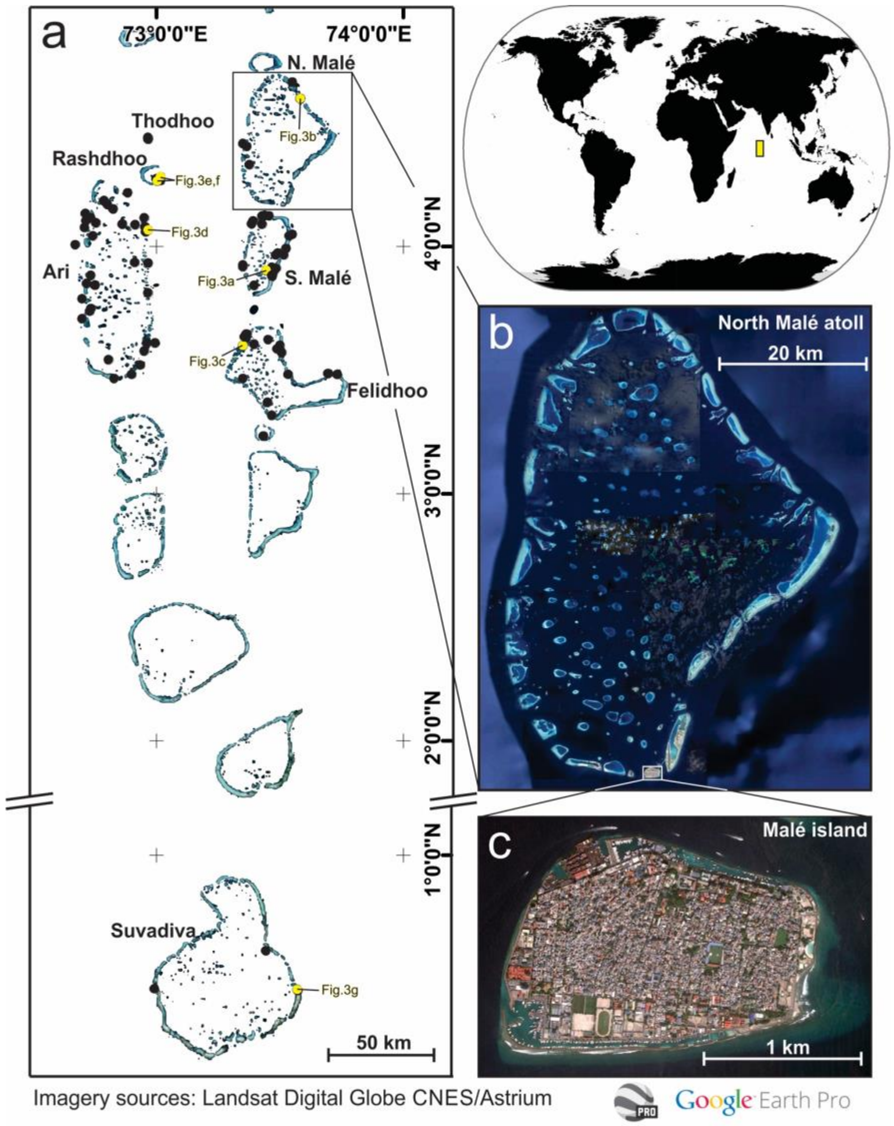

Fig. 1 a) The Maldivian Archipelago. The black dots represent the location of the 112 scuba diving surveys, yellow dots indicate the location of the transects shown in Fig. 4. Note the breaking in the latitude axis b) North Malé atoll. c) Malé Island, around which the 2008 multibeam survey was conducted (see Fig. 5). Map data: Google, Landsat, DigitalGlobe, CNS/Astrium.

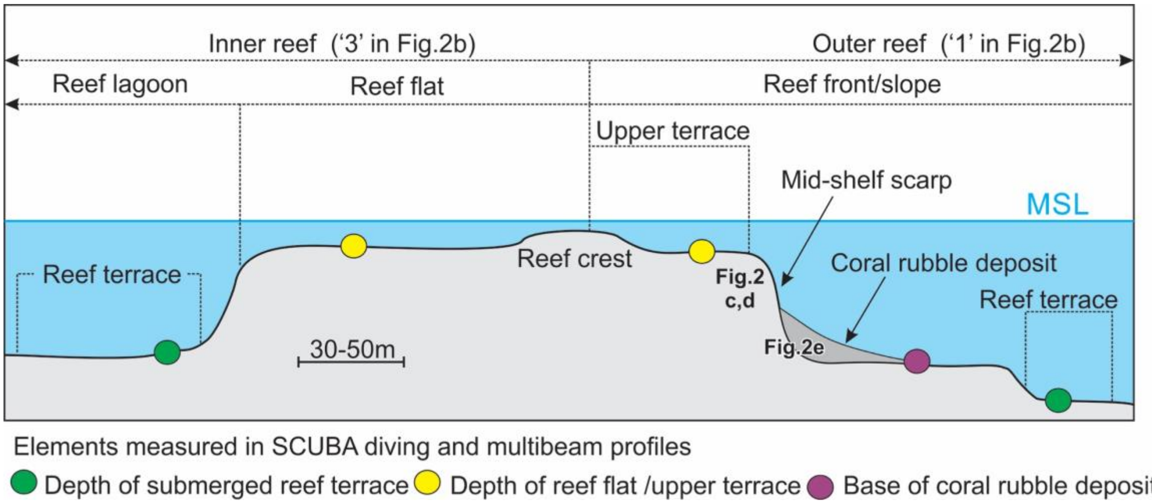

Fig. 2 Terminology related to the reef geomorphic zonation used in this study, and measured depths of important features (colored circles). The terminology has been taken from Blanchon (2011). For field photographs, see Fig. 3.

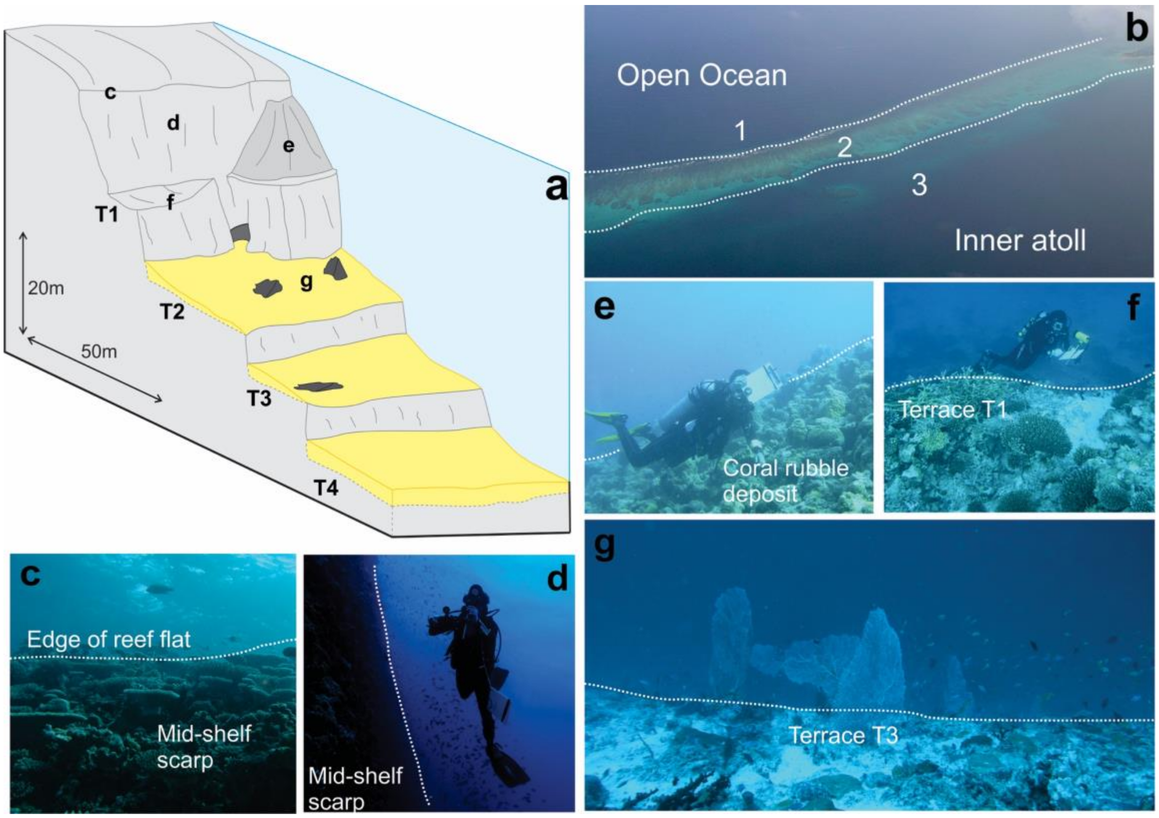

Fig. 3 a) General morphology of inner and outer Maldivian reefs, as derived from scuba diving transects. Note that two more submerged terrace levels were found from multibeam surveys. Letters c to g refer to approximate locations of photos shown in panels c-g. Block diagram derived from an original sketch of V.Parravicini. b) Aerial view of part of a Maldivian Atoll. 1-outer reef; 2-reef flat; 3-inner reef. c) Edge of the modern reef flat at 7 m (Gulhi Kuda Giri, S. Malé). d) Mid-shelf scarp slope between the edge of the modern reef flat and T1 (Boldhuffaru outer reef, S. Malé). e) Accumulation of coral rubble on top of T1. Slope is around 25-30°. The base of this coral rubble deposit is at 23 m (Thoddhoo outer reef). f) Outer edge of T1 (Bodhofoludhoo, Ari). g) Outer edge of T3 (Thoddhoo outer reef).

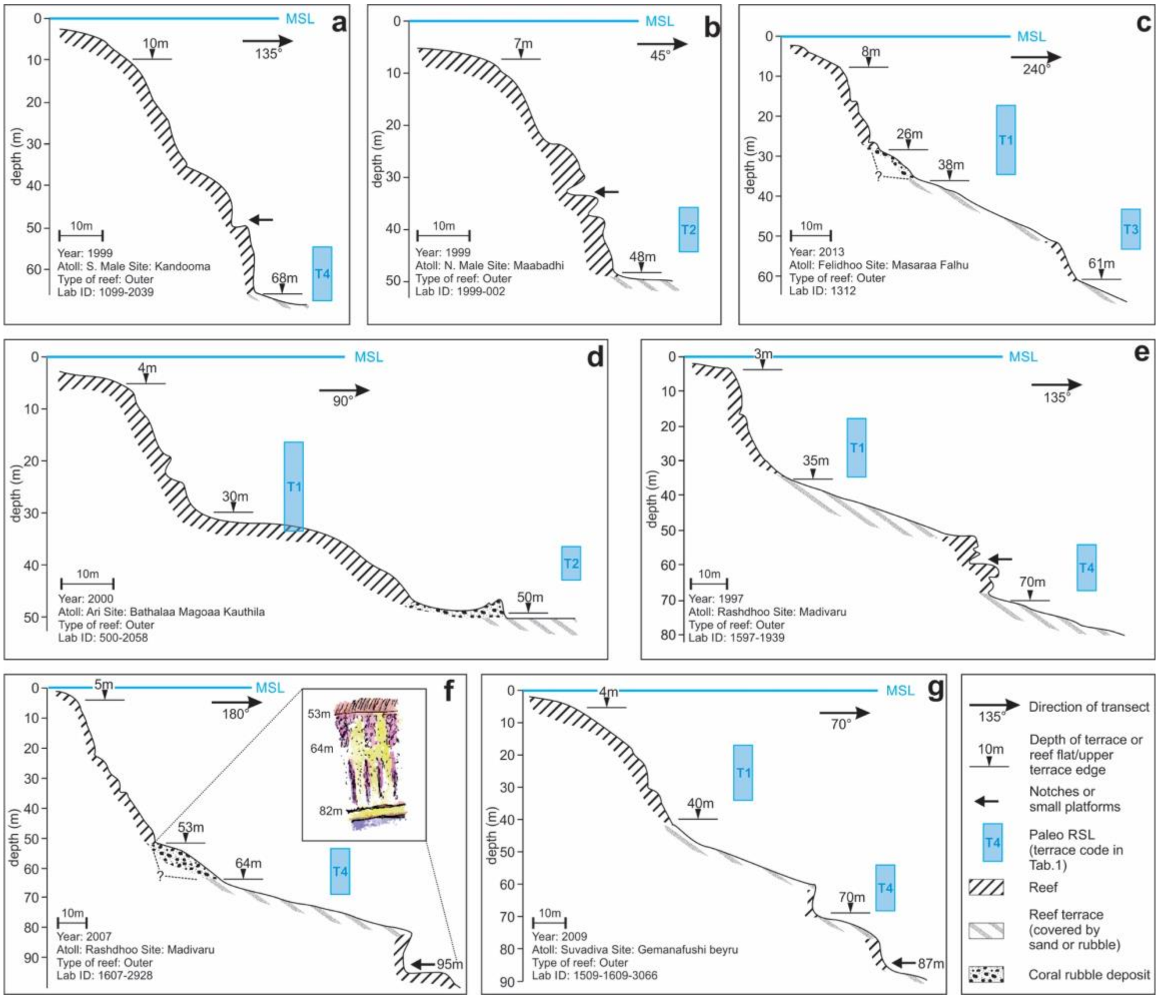

Fig. 4 a-g) Cross-profiles obtained from scuba diving transects. Location for each panel is shown in Fig. 1a. The blue bands represent the calculated paleo sea level from Table 1. In the panel f), the box on the upper right represents the planar view of a tract of the reef between 53 and 82 m drawn during a deep scuba dive by C.N.Bianchi.

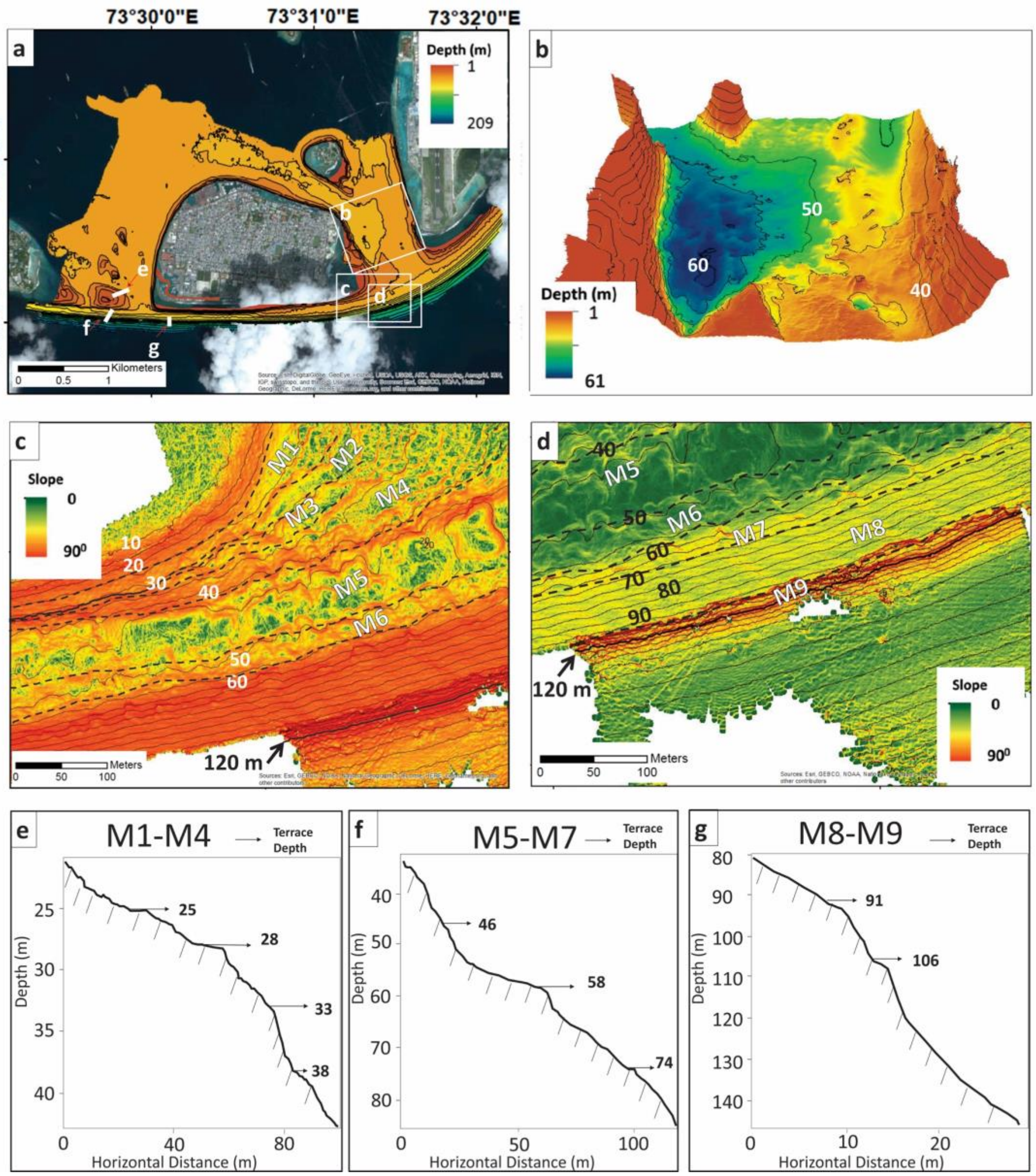

Fig. 5 a) Bathymetric map of Male Island derived from multibeam surveys, with locations of b, c, d, e, f, and g panels. b) Oblique view displaying oval depressions between 50 and 60 m depth, interpreted as sinkholes formed during time of subaerial exposure. c) Slope map illustrating terraces from M1 to M6. d) Slope map illustrating terraces from M5 to M9, separated by steep cliffs. A total of two types of color stretch schemes were used to produce the slope maps: histogram equalize (illustrate better shallow terraces) and percent clip (illustrate better deeper terraces). e), f) and g) Cross profiles show casing terraces M1-M4, M5-M7, and M8-M9. Due to

sediment burial, a continuous slope profile does not show all the terraces and, therefore, three different cross profiles are chosen. These profiles are located in areas of strong currents and thus less masked by sediment deposits. The base of the reef slope is shown by the arrows in (c) and (d) at ~120 m depth.

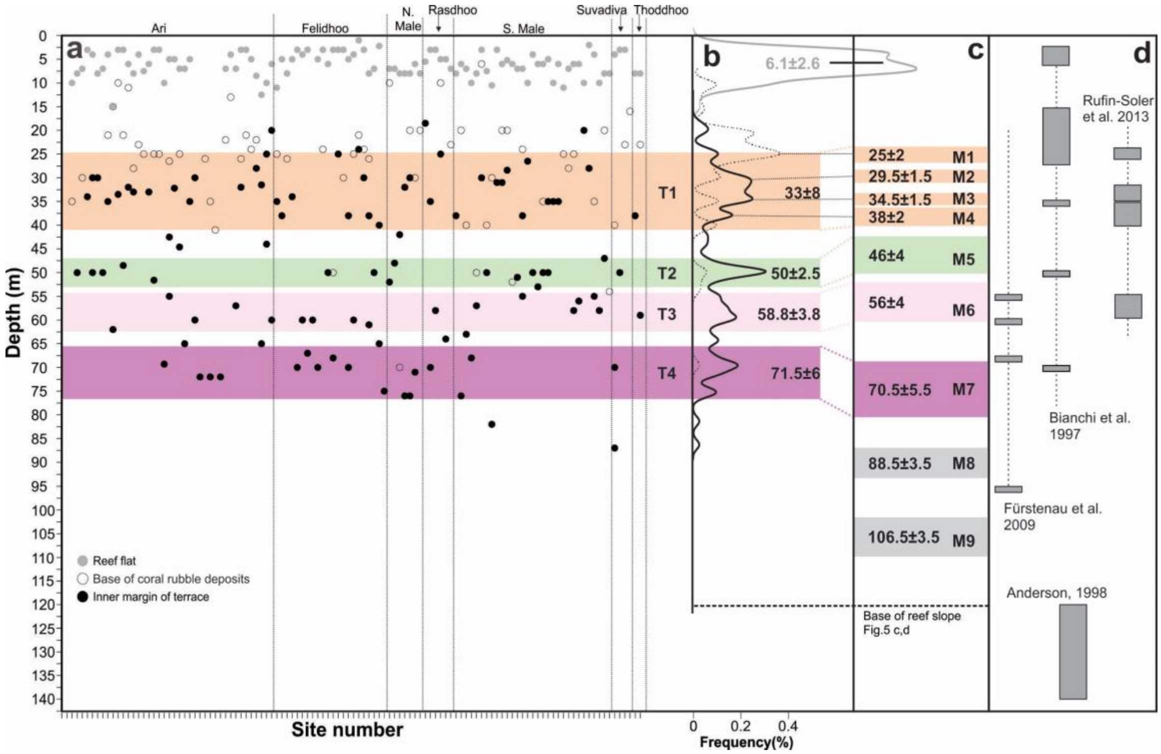

Fig. 6 a) Depth of reef flat/upper terrace (gray circles), of reef terraces (black circles) and of the base of coral rubble deposits (white circles) for each scuba diving transect (see Supplementary Data). b) Relative frequency of terraces plotted by depth, with modal depths of most recurrent terrace levels and associated ranges (black line). The dashed line indicates rockfalls identified at the toe of the reef slope, the gray line indicates the depth of the reef flat/upper terrace edge. c) Terraces M1-M9 identified through multibeam bathymetry dataset, Malé Island. d) Depth of terrace levels identified in the Maldives by previous studies.

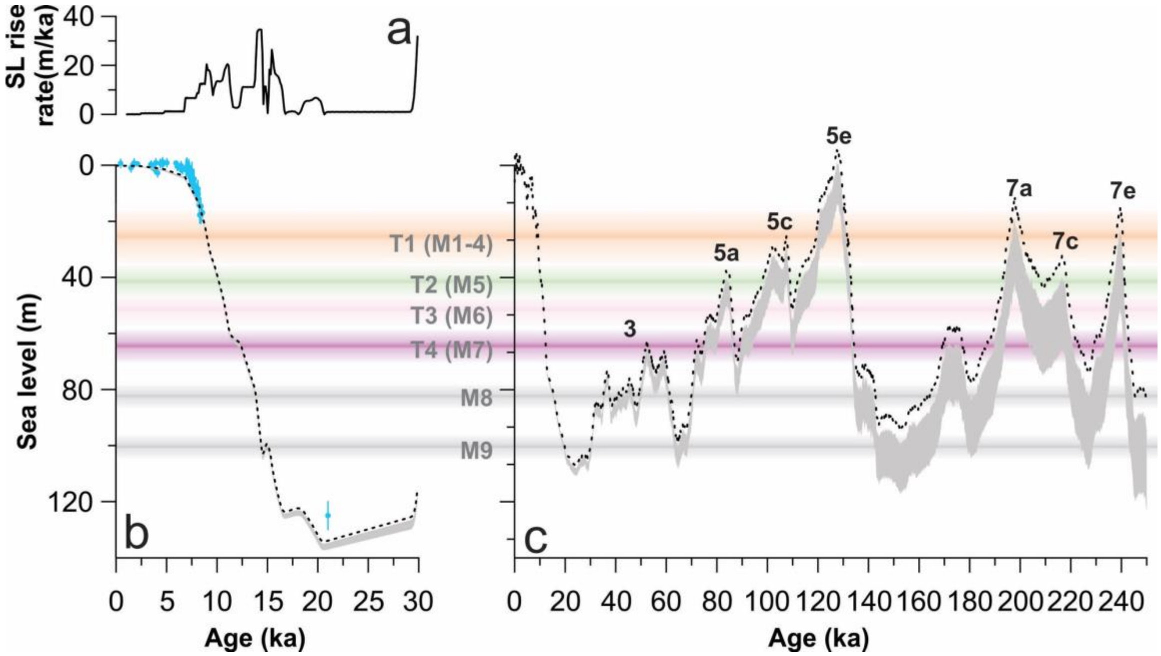

Fig.7 Sensitivity of the paleo relative sea level (RSL) calculation to possible perturbations on the measured reef terrace depth. 1 – no perturbations considered, as in this study; 2 – the measured depth is lower than the original inner margin depth due to reef building since the formation of the inner margin; 3 – the measured depth is higher than the original inner margin depth (green circle) due to erosion since the formation of the inner margin. The lower panel indicates how each case would influence the paleo RSL calculation and associated uncertainties.

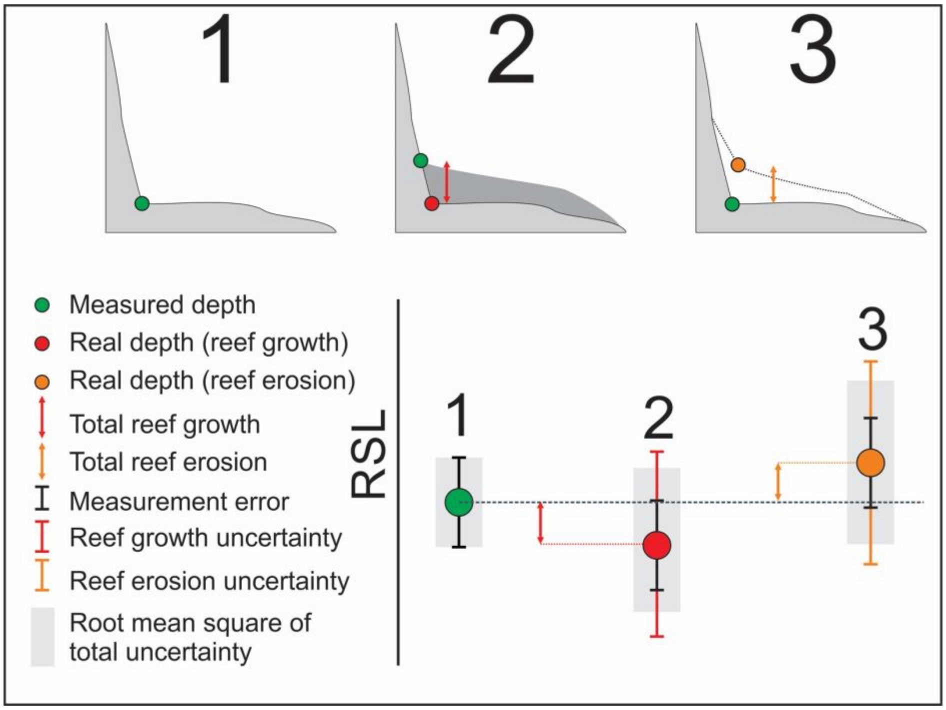

Fig.8 a) Rates of eustatic sea-level (ESL) rise since the Last Glacial Maximum. b) Eustatic sea-level changes since the Last Glacial Maximum. The blue dots represent dated relative sea-level (RSL) index points in the Maldives. c) Eustatic sea-level changes in the last 250 ka. Colored bands represent the paleo RSL inferred from Maldivian terraces (same color code as in Fig. 6c). The dashed line in both graphs represents ESL from Lambeck et al. (2014) (panel b) and Grant et al. (2014) (panel c). The gray band in both graphs shows the Relative Sea Level calculated for the Maldives adding a constant subsidence rate between 0.035 $m{\cdot}ka^{-1}$ to 0.15 $m{\cdot}ka^{-1}$. Neither panel b nor c take into account the possible departures from eustasy caused by glacial isostatic adjustment (GIA) in the Maldives, which are discussed in the text.

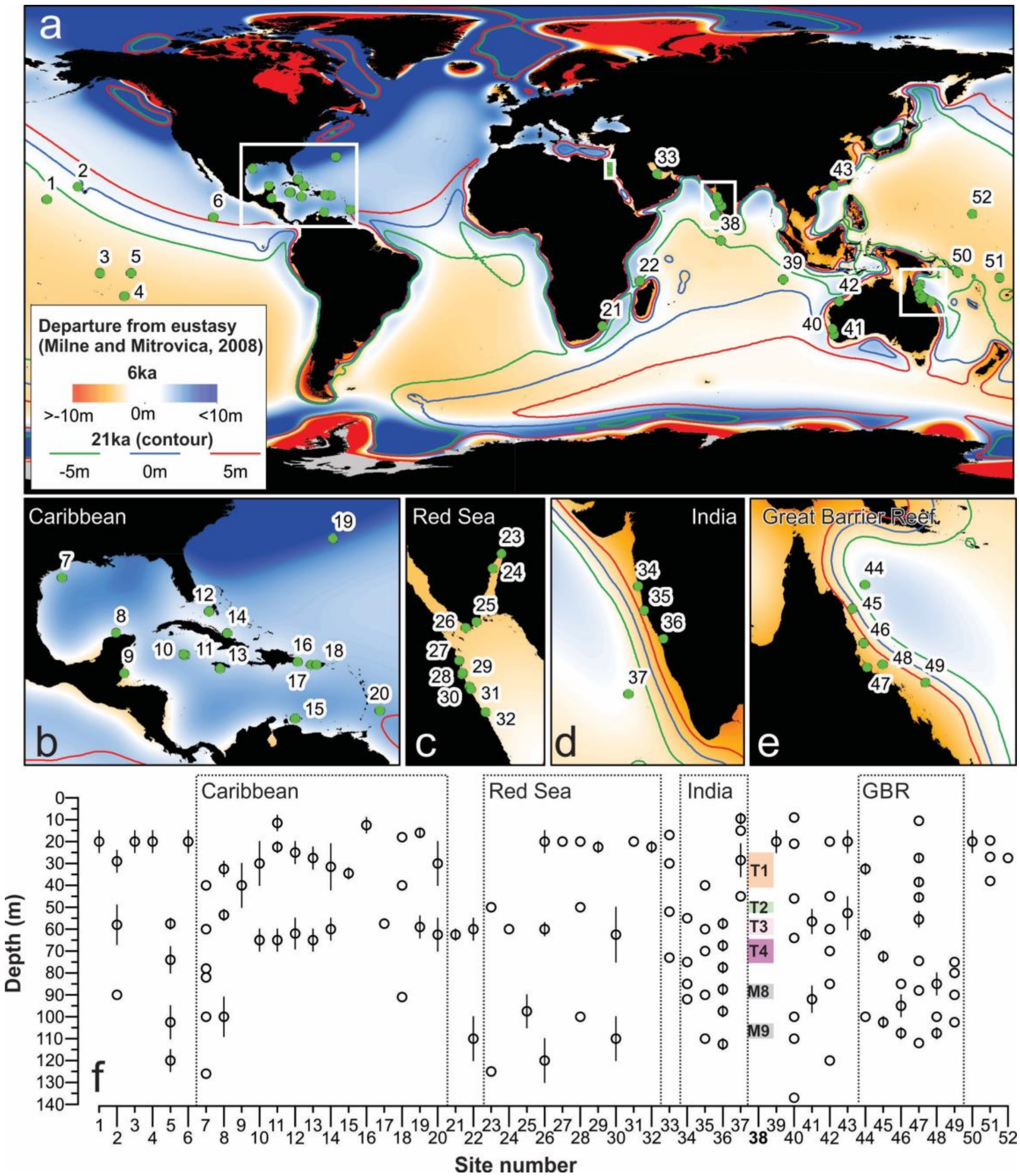

Fig. 9 a) Sites where submerged reef terraces have been reported* (see Supplementary Materials for details). b-e) Detailed view of, respectively: the Caribbean region, the Red Sea region, the Indian region, the Great Barrier Reef region. f) Comparison between the reported depths of reef terraces and the levels found in the Maldives. The background of panels a to e represents the departure from eustasy at 6 ka due to GIA, as calculated by Milne and Mitrovica (2008).

Contours represent the same at 21 ka. *Sites and references (see Supplementary Data for more details): **1 - Johnston Atoll, USA** (Keating, 1985 in Blanchon, 2011); **2 - Ohau, Hawaii, USA** (Fletcher and Sherman, 1995); **3 - Caroline Island, Kiribati** (Tracey, 1968 in Blanchon, 2011); **4 - Tuamotus and Society Islands, French Polynesia** (Newell, 1956 and Chevalier et al., 1968 in Blanchon, 2011); **5 - Marquesas foreslopes (French Polynesia)** (Cabioch et al., 2008); **6 - Clipperton Island, France overseas** (Glynn et al., 1996 in Blanchon, 2011); **7 - Gulf of Mexico, USA** (Poag, 1973); **8 – Yucatan, Mexico** (Logan, 1962); **9 - Belize** (James and Ginsburg, 1979 in Blanchon and Jones, 1995); **10/11 - Grand Cayman** (Rigby and Roberts, 1976 in Blanchon and Jones, 1995); **12 - Great Bahama Bank, Bahamas** (Hine and Neumann, 1977 and Wilber et al., 1990 in Blanchon and Jones, 1995); **13 - Jamaica** (Goreau and Land, 1974, Liddell et al., 1984 and Digerfeldt and Hendry, 1987 in Blanchon and Jones, 1995); **14 - Cuba** (Kühlmann, 1970 in Blanchon and Jones, 1995); **15 - Curacao, Netherland Antilles** (Focke, 1978); **16 - Dominican Republic** (Barrett, 1962); **17/18 - Puerto Rico** (Morelock et al., 1983 and Kaye, 1959a,b); **19 - Bermuda** (Stanley and Swift, 1968); **20 - Barbados** (Acker, 1987 and Macintyre, 1967 in Blanchon and Jones, 1995); **21 - Kwa Zulu Natal, South Africa** (Green et al., 2014); **22 - Mayotte Comoro Islands** (Dullo et al., 1998); **23 – Eilat, Israel** (Reches et al., 1987); **24/32 - Egypt** (Reiss and Hottinger, 1984; Fricke and Landmann, 1983; Gvirtzman, 1994; Moawad, 2013); **33 - Persian Gulf, Qatar** (Houbolt, 1957 in Wagle et al., 1994); **34/36 - India** (Nair, 1974; Vora and Almeida, 1990; Wagle et al., 1994); **37 - Laccadive Islands** (Siddiquie, 1975); **38 - Maldives** (This study); **39 - Cocos (Keeling) islands** (Williams, 1994 in Blanchon, 2011); **40 - Western Australia** (Carrigy and Fairbridge, 1954 in Wagle et al., 1994); **41 - Rottnest Island, Australia** (Collins, 1988); **42 - NW Shelf, Australia** (Hengesh et al., 2011); **43 - South China Sea, China** (Wenke et al., 1982 in Wagle et al., 1994); **44/49 - Great Barrier Reef, Australia** (Sarano and Pichon, 1988; Abbey et al., 2011; Johnson and Searle, 1984); **50 - Solomon Islands** (Stoddart, 1969b in Blanchon, 2011); **51 - Alexa Bank, Melanesia** (Fairbridge and Stewart, 1960); **52 - Bikini, Marshall Islands** (Tracey et al., 1948).